



# Review of pore network modelling of porous media: experimental characterisations, network constructions and applications to reactive transport

DOI:

[10.1016/j.jconhyd.2016.07.002](https://doi.org/10.1016/j.jconhyd.2016.07.002)

## Document Version

Accepted author manuscript

[Link to publication record in Manchester Research Explorer](#)

## Citation for published version (APA):

Xiong, Q., Baychev, T., & Jivkov, A. (2016). Review of pore network modelling of porous media: experimental characterisations, network constructions and applications to reactive transport. *Journal of Contaminant Hydrology*, 192, 101-117. <https://doi.org/10.1016/j.jconhyd.2016.07.002>

## Published in:

Journal of Contaminant Hydrology

## Citing this paper

Please note that where the full-text provided on Manchester Research Explorer is the Author Accepted Manuscript or Proof version this may differ from the final Published version. If citing, it is advised that you check and use the publisher's definitive version.

## General rights

Copyright and moral rights for the publications made accessible in the Research Explorer are retained by the authors and/or other copyright owners and it is a condition of accessing publications that users recognise and abide by the legal requirements associated with these rights.

## Takedown policy

If you believe that this document breaches copyright please refer to the University of Manchester's Takedown Procedures [<http://man.ac.uk/04Y6Bo>] or contact [uml.scholarlycommunications@manchester.ac.uk](mailto:uml.scholarlycommunications@manchester.ac.uk) providing relevant details, so we can investigate your claim.



1                   **Review of pore network modelling of porous media: experimental**  
2                   **characterisations, network constructions and applications to reactive transport**

3  
4                   Qingrong Xiong, Todor G Baychev, Andrey P Jivkov

5                   Modelling & Simulation Centre and Research Centre for Radwaste &  
6                   Decommissioning, School of Mechanical Aerospace & Civil Engineering  
7                   The University of Manchester, Oxford Road, Manchester M13 9PL, UK

8  
9                   **Abstract**

10 Pore network models have been applied widely for simulating a variety of different  
11 physical and chemical processes, including phase exchange, non-Newtonian  
12 displacement, non-Darcy flow, reactive transport and thermodynamically consistent oil  
13 layers. The realism of such modelling, i.e. the credibility of their predictions, depends to  
14 a large extent on the quality of the correspondence between the pore space of a given  
15 medium and the pore network constructed as its representation. The main experimental  
16 techniques for pore space characterisation, including direct imaging, mercury intrusion  
17 porosimetry and gas adsorption, are firstly summarised. A review of the main pore  
18 network construction techniques is then presented. Particular focus is given on how  
19 such constructions are adapted to the data from experimentally characterised pore  
20 systems. Current applications of pore network models are considered, with special  
21 emphasis on the effects of adsorption, dissolution and precipitation, as well as biomass  
22 growth, on transport coefficients. Pore network models are found to be a valuable tool  
23 for understanding and predicting meso-scale phenomena, linking single pore processes,  
24 where other techniques are more accurate, and the homogenised continuum porous  
25 media, used by engineering community.

26  
27                   **Keywords: Porous media; Reactive transport; Pore network model**

1  
2  
3  
4  
5  
6  
7  
8  
9  
10  
11  
12  
13  
14  
15  
16  
17  
18  
19  
20  
21  
22  
23  
24  
25  
26  
27  
28  
29  
30  
31  
32

**1 Introduction**

Flow and transport phenomena in porous media play an important role in many diverse fields of science and technology. For example, radioactive waste management is one of the most pressing problems facing the world today, because of the longevity of radionuclide and the possibility of their transport to the surface environment. For long-term performance assessment of nuclear repositories, knowledge concerning the transport of radionuclide in the back-fill material is required. One porous medium, bentonite, is presently considered as the best candidate for the high level waste disposal, due to its large specific surface area, high ion-exchange capacity, and sorption affinity for organic and inorganic ions. Sorption onto bentonite plays an important role in retarding the migration of radionuclide from a waste repository (Bourg et al., 2003; Bourg et al., 2006; Bradbury and Baeyens, 2003). Another field where such knowledge is highly demanded is the construction industry. Building materials such as bricks, concrete and sandstone all are porous. These materials may interact with their environment leading to degradation of the structures with time. A specific example is that the constituent ions in the hydrated cement paste matrix may leach out from the concrete and cause the concrete structure to become weak. Degradation processes like this strongly relate to the transport phenomena in concrete. Transport mechanisms involved in the degradation processes include: permeation of water or aqueous solutions, diffusion of gaseous compounds and sorption of ionic contaminated water. In such a case, transport properties in these porous media are usually considered as indicators for evaluating the durability and ultimately predetermining the service life of these structures (Zhang et al., 2013; Zhang et al., 2014, (Wang et al., 2015a; Wang et al., 2015b; Zhang et al., 2013). Another example is the contaminated underground water transport, which is controlled by a variety of transport mechanisms including permeation, diffusion and dispersion (McCarthy and Zachara, 1989).

There are several challenges in analysing transport in porous media. Firstly, the intricacy of the pore structure makes the transport processes in porous media very complex. Pores tend to have irregular surfaces and some of them even make dead ends.

1 These factors influence the flow and transport behaviour significantly. Another  
2 difficulty of studying transport processes in porous media is the evolution of pore  
3 structure during their service or operation, etc. These changes may result from chemical,  
4 electrochemical or bacterial effects as well as from mechanical damage, such as micro  
5 cracking. The evolution of the pore space may lead to changes in the macroscopic  
6 transport properties, such as permeability and diffusivity. Furthermore, the transport  
7 properties in porous media are a function of types of species in solution and the phase  
8 (Appelo et al., 2010). Finally, many reactive pore network models (Li et al., 2006;  
9 Raouf et al., 2012) employ a reaction rate or mass transfer coefficient measured in a  
10 macroscopic experiment. For example, these authors determine reaction rate  
11 coefficients from spinning disk, flow-through reactor, or continuous fluidized bed  
12 reactor experiments. These results may not be applicable to reaction rates in individual  
13 pores, as the smaller scale magnifies the effects of mass transfer resistance and  
14 concentration gradients. Raouf et al. (2010) demonstrated the importance of  
15 incorporating kinetics developed for the pore scale, rather than relying on macroscopic  
16 averages.

17

18 Due to the complexity of the pore structure and the change of the environmental  
19 conditions, a great deal of experimental, theoretical and numerical approaches have  
20 been proposed and developed to study transport processes through porous media during  
21 the past decades (Abichou et al., 2004; Aytas et al., 2009; Boulton et al., 1998; Ghassemi  
22 and Pak, 2011; Kohler et al., 1996; Li et al., 1992; Ren et al., 2009; Tsai and Chen,  
23 1995; Wang et al., 2005). Field and reactive transport experiments as well as studies  
24 involving X-ray, SEM, TEM etc. are usually expensive and time consuming. The  
25 measurements are highly sensitive to the material composition, sample preparation,  
26 methodology and testing environment. Analytical solutions are typically restricted to  
27 problems with assumed homogeneous properties and specific boundary conditions,  
28 some of which have limited practical relevance or are complicated to evaluate.

29

30 Pore-scale simulations have improved the understanding of large-scale natural processes  
31 and informed large-scale geotechnical applications. Their importance comes from the  
32 fact that they can produce rather cost-effective and accurate predictions for local

1 transport (diffusion/permeation), and at the same time allow for systematic variations of  
2 the system's parameters (pore space geometries, fluid properties, and boundary  
3 conditions) to assess their impact, which is much more difficult to achieve than with  
4 experiments (Meakin and Tartakovsky, 2009). With pore-scale models one can make  
5 improved assessments of macroscopic transport properties by varying the pore space  
6 structure parameters. This offers a way to understand the scale dependence of  
7 continuum transport parameters. Such scale dependence cannot be captured by an  
8 effective medium Darcy approach. The pore-scale modelling is dominated by particle-  
9 based methods. These include the promising lattice Boltzmann method (Hao and Cheng,  
10 2010; Zhang et al., 2014; Zhang et al., 2013) and smoothed particle hydrodynamics  
11 (Tartakovsky and Meakin, 2006; Tartakovsky et al., 2007; Zhu and Fox, 2002).

12  
13 The particle methods, while suitable for pore-scale analyses, become inefficient at the  
14 meso-scale, e.g. when the system requiring analysis has tens or hundreds interconnected  
15 pores in each direction (Tartakovsky et al., 2007). Further, these methods are time  
16 consuming and only very limited pore volumes can be addressed. In order to increase  
17 the pore volume with affordable computational resources and a reduced impact on the  
18 reliability of the results, the pore network model (PNM) approach has been used to  
19 study reactive transport phenomena. At the meso-scale the classical macroscopic  
20 equations, such as the Darcy law, are yet not needed, i.e. fluid flow and solute transport  
21 processes are simulated directly in the pores, but the precise particle dynamics, which  
22 can be analysed by particle methods, is not accounted for. This is done by creating a  
23 virtual representation of the porous medium consisting of pore bodies and pore throats  
24 of different sizes (the "geometry" of the porous medium), connected to each other as  
25 required (the "topology" of the porous medium). It is then possible to simulate the fluid  
26 flow and solute transport process of interest at the meso-scale through this network,  
27 with the relevant physics implemented on a pore-to-pore basis. The first network model  
28 was constructed by Fatt (Fatt, 1956) who exploited the analogy between flow in porous  
29 media and a random resistor network. Afterwards, the models have grown in  
30 sophistication and now can deal with irregular lattices, wetting layer flow, arbitrary  
31 wettability and any sequence of displacement in two- and three-phase flow, as well as a  
32 variety of different physical processes, including phase exchange, non-Newtonian

1 displacement, non-Darcy flow, reactive transport and thermodynamically consistent oil  
2 layers, etc., (Balhoff and Wheeler, 2009; Blunt et al., 2002; Lopez et al., 2003;  
3 Ryazanov et al., 2009; Yiotis et al., 2006).

4  
5 Compared to the pore-scale modelling methods, such as the lattice-Boltzmann and  
6 particle methods, pore-network models take less time to compute and require less  
7 computer capacity due to the inherent simplifications of the pore-space in the  
8 construction of the model. Pore network simulations are much less computationally  
9 demanding than direct methods. This allows researchers to incorporate more  
10 heterogeneity in modelling larger rock volumes. As natural geological media can be  
11 heterogeneous on all length scales, this is an important advantage of pore network  
12 modelling. Pore network models have been used extensively to simulate multiphase and  
13 single-phase fluid flow in porous media, and these models will continue to provide  
14 important insight and information in the future. However, pore network models are  
15 usually constructed based on simplified geometry due to the lack of experimental  
16 resolution in pore space characterisation. This could make the predictions of transport  
17 properties less credible. The greatest challenge in obtaining credible results is the  
18 identification of features/phenomena relevant to the modelled process and neglecting  
19 the rest to reduce the computational load. For example, to compute the single phase  
20 flow field, it is necessary that the principal connected pore space is modelled; while the  
21 very small pores below the image resolution can be neglected as they make little  
22 contribution to the overall behaviour (Blunt et al., 2013).

23  
24 The suitability of the pore-scale modelling techniques for a given application depends  
25 on the governing equations, the underlying assumptions for the pore-scale flow and  
26 transport equations, as well as the length-scales of the (computational) domain, etc.  
27 While the lower scale limit of a pore-scale technique is determined by the scale of the  
28 governing equations, the upper scale limit is set by the computational power. In this  
29 review we focus on the pore network models with comprehensive account for the  
30 methods for obtaining pore space information, constructing pore networks and the  
31 application of pore network models to reactive transport in porous media.

## 2 Characterisation of pore space information

For pore network model construction, the geometry and topology of the pore space are required. There are several ways to characterize the pore space. One is imaging techniques such as producing 3D images by mapping the real interior structure of original samples (the destructive approach of cutting and stacking serial 2D sections, confocal laser scanning microscopy and non-destructive X-ray micro-tomography (micro-CT)), and constructing synthetic 3D rock images from high resolution 2D thin sections using statistical methods or geological process simulation. Other non-destructive approaches are mercury intrusion porosimetry and gas adsorption, which produce pore size distribution and surface area, but not the full connectivity. The main methods for space characterisations are reviewed in this section.

### 2.1 Imaging techniques

#### 2.1.1 X-ray computed micro-tomography (micro-CT)

Micro-CT is a non-destructive and non-invasive imaging technique used to characterize cross-sectional and three-dimensional internal structures (Hazlett, 1995; Lindquist et al., 1996; Schlüter et al., 2014).

To image geological porous materials at the micro-scale, three types of micro-CT systems are in common use: medical CT, industrial X-ray generation tube and synchrotron micro-tomography. They primarily differ in X-ray energy and source, means of sample manipulation and detector geometry. Although the best image resolution reported in the literature is from synchrotron micro-CT, the samples need to be relatively small to achieve these resolutions. This may result in poor statistical representation of the bulk material. Typical spatial resolution that medical CT systems can achieve is between 200 to 500  $\mu\text{m}$ , industrial systems range from 50 to 100  $\mu\text{m}$  and synchrotron based CT systems can reach from 1  $\mu\text{m}$  to 50  $\mu\text{m}$  (Wildenschild et al., 2002a). Presently, laboratory systems with genuine submicron capabilities exist, some with voxel resolution of 20nm, providing spatial resolution of 50-60 nm. Three main

1 configurations are used in systems that seek submicron resolution; a good review can be  
2 found in (Schlüter et al., 2014; Withers, 2007). Specific details of these imaging  
3 techniques and their evolution can be found in previous reviews (Blunt et al., 2013;  
4 Ketcham and Carlson, 2001).

5  
6 It should be noted that X-ray CT may obscure significant features or misinterpret  
7 attenuation values of a single material in different image sections resulting in  
8 complicated quantitative image analysis (Ketcham and Carlson, 2001). Commonly  
9 experienced problems include beam hardening, high-frequency noise, scattered X-rays,  
10 defective detector pixels or poorly centered samples (Ketcham and Carlson, 2001;  
11 Wildenschild et al., 2002b). In addition, there might be errors and distortions arising  
12 from the CT reconstruction (Ketcham and Carlson, 2001). These problems cannot be  
13 completely avoided, but can be alleviated by careful detector calibration, metal filters  
14 and sample centring. Application of wedge calibration and dual energy scans (Rebuffel  
15 and Dinten, 2007) can also reduce beam hardening effects, but these techniques are  
16 rarely implemented in standard scanning procedures (Ketcham and Carlson, 2001).

#### 17 18 2.1.2 Focused ion beams and Scanning electron microscopy

19  
20 Focused ion beams (FIB) and Scanning electron microscopy (SEM) are destructive  
21 imaging techniques. SEM is a useful technique for extracting two-dimensional (2D)  
22 images of the microstructures but does not provide the third spatial component of the  
23 sample, which is important to find interconnected regions and pore volumes, shapes and  
24 sizes. Depending on the instrument, the resolution achieved can be between 1 and 20  
25 nm. The world's highest resolution conventional SEM can reach a point resolution of  
26 0.4 nm by utilising a secondary electron detector ([http://www.nanotech-  
27 now.com/news.cgi?story\\_id=42612](http://www.nanotech-now.com/news.cgi?story_id=42612)). FIB is a well-established technique to acquire very  
28 high-resolution three-dimensional images, typically just a few micro-meters across  
29 (Curtis et al., 2010; Lemmens et al., 2010; Tomutsa et al., 2007). This technique can  
30 achieve less than 1 nm imaging resolution  
31 (<http://www.fibics.com/fib/tutorials/introduction-focused-ion-beam-systems/4/>).

32 Although this method provides a great potential for imaging hydrocarbon bearing rocks



1 at high resolution and produces images with better quality than the electron beam  
2 imaging due to less charging of the surface, it is still significantly time consuming due  
3 to the refocusing between milling and imaging as well as the sample repositioning  
4 (Tomutsa et al., 2007). Due to these limitations, this technique exposes only small areas  
5 of observation and cannot provide adequate sampling to characterize the sample, e.g.  
6 from a shale reservoir.

7

8 The combination of FIB and SEM (FIB-SEM) is usually used to compute micro-  
9 structural properties of porous media. This combination allows for the observation of  
10 fine macro-pores and meso-pores within the porous medium (Keller et al., 2011;  
11 Tomutsa et al., 2007). This method can typically achieve voxel dimensions of tens of  
12 nanometers, thus allowing for analysing volumes of around  $(10 - 30)^3 \mu\text{m}^3$  within  
13 practical measuring time (Michael D. Uchic, 2007) .

14

15 Multi-scale imaging capabilities, such as the development and integration of a range of  
16 experimental and computational tools, can facilitate probing the structure of materials  
17 across various scales in an integrated fashion. Given their important function, multi-  
18 scale imaging capabilities have been an area of focus of several research groups in the  
19 recent years.

20

21 The combination of FIB, SEM and TEM (transmission electron microscopy) is used to  
22 analyse the structure of pore space (Wirth, 2009). For example, the backscattered  
23 scanning electron microscopy (BSEM) and focused ion beam SEM (FIBSEM) have  
24 been utilised to analyse rocks (Sok et al., 2010). These techniques are particularly  
25 suitable for examining carbonates due to their multi-modal pore structure, which can  
26 range from 10 nm to 10 cm. Sok et al (Sok et al., 2010) report on both plug to pore scale  
27 registration in 3D, as well as pore-scale to submicron scale registration of features. The  
28 plug to pore scale approach requires one or more subsets of the sample originally  
29 imaged (at the scale of 4 cm and at 20  $\mu\text{m}/\text{pixel}$ ) which then have to be reimaged with  
30 Micro CT at a smaller sample volume (5 mm and at 2.5  $\mu\text{m}/\text{pixel}$ ). After that the data

1 should be carefully registered and integrated. The pore-scale to submicron scale  
2 registration was done by cutting the subsamples and preparing thin sections from the  
3 original field of view of the Micro CT images. The thin sections were then imaged with  
4 BSEM and registered to the Micro CT image. Finally, in order to estimate reservoir  
5 properties for complex materials, such as carbonate and mudstones, FIBSEM images  
6 were also obtained at voxel resolutions of 50 nm. A longer term goal of Sok et al\_group  
7 is to undertake complete multi-scale registration from the whole core and/or plug scale  
8 through the Micro CT length scale and down to the submicron (SEM or FIBSEM) scale.

### 10 2.1.3 Nuclear magnetic resonance

12 Recent NMR development has demonstrated the use of relaxation, cryoporometry,  
13 spectroscopy, diffusion, and imaging techniques to quantify pore structure (i.e. pore  
14 sized distribution, pore morphology, connectivity etc.), fluid properties, and rock  
15 heterogeneity. The NMR relaxometry poses the least demands on magnetic field quality,  
16 NMR imaging favours magnetic fields linear in space with a constant gradient, and  
17 NMR spectroscopy, places the highest demands on field homogeneity and field stability.

19 Magnetic resonance imaging allows the imaging of the interior of the rocks to obtain the  
20 spatial distribution across a much larger scale (Blümich et al., 2009). Callaghan et al.  
21 (Callaghan, 1993) discovered the diffusion diffraction phenomenon when the gradient  
22 wavelength approaches the characteristic pore size. Since the water molecules in the  
23 porous material will move randomly, they will probe the pore structure. This will  
24 influence the transverse relaxation time. Therefore, NMR can provide information on  
25 the pore-size distribution of a porous material by measuring this transverse relaxation  
26 time. The major advantage of NMR in comparison with classical methods is the short  
27 measurement time. This would allow the analysis of large quantities of samples as  
28 required to characterize a field or catchment-scale hydraulic properties, which are  
29 necessary for risk assessment (e.g., flood forecasting) and management (e.g.,  
30 fertilization and pest control). The determination of pore size distributions by NMR  
31 relaxometry has its own drawbacks. First, the diffusion in induced magnetic field  
32 gradients can shorten transverse relaxation times ( $T_2$ ). This must be checked and can be

1 minimized by choosing sufficiently small echo times or by measuring longitudinal  
2 relaxation ( $T_1$ ). Second, diffusion in internal gradients may affect different modes of a  
3 multimodal relaxation time distribution function in a different way. Third, one must be  
4 aware that the derivation of PSD is always a scaling procedure, which requires  
5 independent determination of the average specific surface area. The reason is that the  
6 relaxation times are controlled by the pore sizes and surface relaxivity, but the average  
7 S/V is controlled by the internal surface area of the porous media. Fourth, the  
8 assumption of the homogeneous distribution of pores and paramagnetic centres and the  
9 calculation of an average surface relaxivity parameter, especially for a multimodal  
10 relaxation time distribution function, leads to an overestimation of the large pores. All  
11 these issues, together with the necessary simplification of pore shape and geometry, can  
12 deviate the calculated pore size distribution from the real one (Stingaciu et al., 2010).

13

14 Nuclear magnetic resonance (NMR) relaxometry uses the random motion of molecules,  
15 whereas cryoporometry uses the melting-point depression of a confined liquid  
16 determining pore size distributions. It is suitable for measuring pore diameters in the  
17 range 2 nm–1  $\mu\text{m}$ , depending on the absorbate. Whilst NMR cryoporometry is a  
18 perturbative measurement, the results are independent of spin interactions at the pore  
19 surface and so can offer direct measurements of pore volume as a function of pore  
20 diameter (Mitchell et al., 2008). NMR cryoporometry (Strange et al., 1993) rely on the  
21 Gibbs–Thomson equation concerning the relationship between the characteristic pore  
22 length scale and the change in the freezing point of the liquid, or melting point of its  
23 solid crystal, due to confinement within the porous matrix. However, the freezing and  
24 melting behaviour of confined liquids/solids is often complex, with the thermodynamic  
25 properties of the confined material being modified from those of the bulk (Christenson,  
26 2001). NMR cryoporometry offers the advantage of a more direct measure of the open  
27 pore volume.

28

29 The pore-size distribution obtained from cryoporometry is the derivative of the total  
30 liquid water content with respect to temperature. Because noise is always present in the  
31 NMR data, the derivative can have an irregular shape for pores having only a minor  
32 contribution to the total signal. However, no a priori shape of a distribution is imposed.

1 On the other hand, the pore-size distribution obtained from relaxometry is the result of a  
2 numerical inverse Laplace transform. This is generally an ill-posed problem and hence  
3 some sort of regularization method is used. The numerical code that we use always  
4 yields a sum of log-normal Gaussian-shaped pore-size distributions. Therefore the shape  
5 of the relaxometry pore-size distribution does not accurately reflect the actual pore-size  
6 distribution. Only the position of the peaks and the total area of the distribution around a  
7 specific peak are relevant parameters in this pore-size distribution (Valckenborg et al.,  
8 2002).

## 10 **2.2 Mercury Intrusion Porosimetry (MIP)**

11  
12 Mercury intrusion porosimetry is by far the most popular method for characterizing  
13 porous materials with pores in the range of 500  $\mu\text{m}$  down to 3nm (Giesche, 2006; León  
14 y León, 1998; Rouquerol et al., 2012). Compared to alternative characterization  
15 methods such as gas sorption, mercury porosimetry covers a much wider pore size  
16 range, while it is based on simpler physicochemical principles and it is much faster in  
17 operation. The most important limitations of the mercury intrusion when applied to  
18 extract pore size distribution of a porous material is that it is based on the assumption  
19 that the porous matrix can be represented by a bundle of cylindrical pores. In extracting  
20 pore size distribution during mercury intrusion, all pores are assumed to be equally  
21 accessible to the exterior mercury reservoir. This assumption can only be met if the pore  
22 structure is represented in the form of a bundle of capillaries or if pore connectivity is  
23 very high. In reality, however, pore network effects can be quite important resulting in  
24 the so-called pore shadowing or ink-bottle phenomenon. In this case, a large pore has  
25 smaller entrances connecting with the mercury reservoir and can only be filled at a  
26 pressure higher than that required by its actual dimensions. Capillary network models of  
27 varying complexity have been used over the past three decades and have been often  
28 quite successful in proving structural characteristics of the porous materials examined  
29 (Ioannidis and Chatzis, 1993a; Kikkinides and Politis, 2014). For obvious reasons this  
30 method could be applied to study only the open porosity features, since the closed pores  
31 are inaccessible to the mercury (Giesche, 2006).

## 2.3 Gas Adsorption

Adsorption behaviour of porous materials is a function of their microstructural characteristics, such as the surface area, types of pores present in the material, topology of the porous network and the available pore volume. Characterisation of porous materials is, therefore, important in the development of adsorption applications. Mercury porosimetry and gas adsorption are determined from surface tension, capillary forces and pressure. The main difference is that with mercury porosimetry, large pores at the intrusion phase are determined first, while with gas adsorption, the smallest pores are measured first at the adsorption phase.

Physical gas adsorption has been used to study the pore characteristics of solid materials and the changes therein upon post-synthesis treatment. Gas adsorption is one of the most popular techniques used to characterize the pore space. It only allows determining the volume of open pores while closed porosity cannot be accessed. The advantage of this technique is that it allows assessing a wide range of pore sizes, covering essentially the completed micro-and meso-pore range in a timely and cost-effective fashion (Thommes, 2010).

Frequently used adsorptives are nitrogen ( $N_2$ ), argon ( $Ar$ ), and  $CO_2$ , depending on the nature of the material (adsorbent) and the information required. Nitrogen at 77 K is considered to be a standard adsorptive for surface area and pore size analysis, but it is meanwhile generally accepted that nitrogen adsorption is not satisfactory with regard to a quantitative assessment of the micro-porosity, especially for micro- pores with widths smaller than 0.7 nm. Consequently, alternative probe molecules have been suggested, e.g., argon and carbon dioxide. For many micro porous systems, argon adsorption at 87.3 K appears to be very useful as  $N_2$  adsorption in microspores occurs at lower  $p/p_0$  values than Ar (Groen et al., 2003; Ravikovitch et al., 2000; Serrano et al., 2009). Despite this advantage, the low pressures induced restricted diffusion prevents argon molecules from entering the narrowest micropores, i.e., pores of widths < ca. 0.45 nm. Furthermore, Ar adsorption at 77 K shows limited application for meso-pore size determination, since the coolant temperature is below the bulk triple point. As a

1 consequence, pore condensation vanishes in case the pore diameter exceeds  
2 approximately 12 nm (Thommes et al., 2002). When compared to nitrogen and carbon  
3 dioxide, it exhibits weaker attractive fluid-pore wall attractions for most adsorbents,  
4 which during adsorption does not give rise to specific interactions (like nitrogen and  
5 carbon dioxide because of their quadrupole moments) with most of surface functional  
6 groups and exposed ions. CO<sub>2</sub> is another usually preferred adsorptive, since these  
7 adsorption measurements are mostly performed at temperatures near ambient, which  
8 will enhance diffusion properties in the highly micro porous system compared to the  
9 low temperatures used in N<sub>2</sub> and Ar adsorption (Rouquerol et al., 2013). A drawback of  
10 CO<sub>2</sub> adsorption at ambient temperature is that in most commonly used equipments,  
11 which predominantly operate in the pressure range of vacuum to 1 bar, only a limited  
12 range of micropores can be measured, unless high-pressure CO<sub>2</sub> adsorption is used  
13 (Cazorla-Amorós et al., 1998; Ravikovitch et al., 2000). While CO<sub>2</sub> adsorption at 273 K  
14 is frequently used for the ultramicropore analysis of carbonaceous materials (Rodríguez-  
15 Reinoso, 2009), it is not a good choice for the pore size analysis of materials with polar  
16 sites, mainly because of the very specific interactions that CO<sub>2</sub> can have with functional  
17 groups on the surface.

18

19 After obtaining the physical adsorption isotherms, the interpretation of experimentally  
20 measured isotherms is required in order to arrive the specific characteristics of the  
21 material (Thommes, 2010). Classical theories include the Brunauer–Emmett–Teller  
22 (BET) method (Brunauer et al., 1938), Barrett–Joiner–Halenda (BJH) (Barrett et al.,  
23 1951), Broekhoff–de Boer (BdB) method (Broekhoff and De Boer, 1967), Horvath–  
24 Kawazoe (HK) model, (Horvath and Kawazoe, 1983), and the Saito–Foley (SF) model  
25 (Saito and Foley, 1991; Saito and Foley, 1995). Typically, these theories involve certain  
26 assumptions, which are not universally applicable. For example, the notion of an  
27 adsorbed monolayer required by the BET theory to assess the surface area is clearly not  
28 applicable to materials with narrow pores and complex energy landscapes. The classical  
29 BJH, based on the Kelvin equation and corrected for multi-layer adsorption, is most  
30 widely used for calculations of the pore size distribution (PSD) over the mesopore and  
31 part of the macropore range. However, the BJH and BdB theories of extracting PSD,  
32 based on a description of a porous material as a collection of cylindrical or slit pores,

1 are not appropriate for zeolites, metal organic frameworks, polymers etc. The  
2 conventional HK model for slit-shaped pores and SF model for cylindrical pore  
3 geometry are mainly applied for micro-pore size calculations (Groen et al., 2003). Such  
4 approaches allow for obtaining the pore size distribution in addition to the pore volume,  
5 but rely on similar macroscopic and thermodynamic assumptions concerning the nature  
6 of confined adsorbate. This leads to inaccurate determination of the pore size and  
7 volume. New models based on non-local density functional theory (NLDFT) and  
8 molecular simulations were developed (Lukens et al., 1999; Neimark and Ravikovitch,  
9 2001; Neimark et al., 2000). It has been demonstrated that the application of these novel  
10 theoretical and molecular simulation based methods leads to: (i) a much more accurate  
11 pore size analysis (Neimark and Ravikovitch, 2001; Thommes et al., 2006), and (ii)  
12 allows performing pore size analysis over the complete micro/mesopore size range  
13 (Thommes et al., 2006). Currently there are methods for pore size quantification based  
14 on NLDFT and molecular simulations, which are commercially available and applicable  
15 to a range of adsorptive/adsorbent systems. They include hybrid methods that assume  
16 various pore geometries for the micro- and meso-pore size range, as it can be found for  
17 materials with hierarchical pore structures.

18

19 Previously published review on the use of gas adsorption for characterization of porous  
20 materials hardly comment on these phenomena (Sing, 2001). One drawback is that the  
21 process could be very time consuming, but the determinable pore diameter is from 0.3  
22 to 300 nm, a range not completely covered by mercury porosimetry.

23

### 24 **3 Pore network model construction**

25

26 The different experimental techniques for pore space characterisation present different  
27 limitations to the way representative pore networks can be constructed. For example, if  
28 a 3D image is available (experimental or synthetically generated), pore networks can be  
29 constructed directly from this image, assuming what is considered to be a pore and what  
30 to be a throat between pores. The need for up-scaling from the typically small imaged  
31 volume to larger domains leads to the need for construction of statistically  
32 representative networks. This requires analysis of the image to extract size distributions

1 of pores and throats and their connectivity. However, if the experimental data comes  
2 from non-imaging techniques such as mercury intrusion porosimetry and gas adsorption  
3 where not all pore space characteristics are readily available, regular pore network  
4 construction approach is usually applied with assumed connectivity (Jivkov and Olele,  
5 2012).

6  
7 To a large extent the success of pore network models depends on the way they represent  
8 the real pore space in terms of its geometrical and topological characteristics for a given  
9 application. Previous works have clearly demonstrated the importance of the geometric  
10 properties of the porous media, such as the locations of pores and throats, the  
11 distributions of sizes and shapes of pores and throats (Blunt et al., 1992; Knackstedt et  
12 al., 1998; Oren, 1994)). Most early works on pore-scale modelling assumed that the  
13 throats were cylinders with a circular cross-section or considered to be zero-volume  
14 connections between pore chambers. Pores were either not modelled explicitly at all  
15 (they simply represent throat junctions), or were spherical, cubical or cylindrical in  
16 shape. These methods have been applied to study the convection, transient and steady-  
17 state diffusion, permeability, etc. (Bryntesson, 2002; Jivkov and Xiong, 2014; Laudone  
18 et al., 2008; Meyers and Liapis, 1999; Meyers et al., 2001)). Recent advances have  
19 allowed modelling a degree of irregularity in pore cross-sectional shape that was not  
20 available in earlier PNM (Al-Gharbi and Blunt, 2005). For some applications, such as  
21 multiphase flow, it may be necessary to pay specific attention to the local morphology  
22 of the throats (Fenwick and Blunt, 1998; Gao et al., 2012; Hui and Blunt, 2000; Man  
23 and Jing, 1999; Payatakes et al., 1973). For others, such as longer-scale permeability or  
24 diffusivity predictions, the throats could be considered as straight channels with locally  
25 averaged cross sections (De Josselin de Jong, 1958). In the latter case, the variability in  
26 throat morphologies becomes of secondary importance and the transport is controlled  
27 predominantly by the sizes and spatial positions of pores, and the connectivity of the  
28 pore set via throats with different permittivity. In addition, the models have to reflect  
29 basic topological properties, such as average pore coordination number and pore  
30 coordination spectrum. The effects of the average pore coordination on transport  
31 coefficients have been demonstrated in a number of works (Meyers and Liapis, 1999;  
32 Raoof and Hassanizadeh, 2010a). The pore spectrum represents the relative number of



1 pores coordinated by different number of throats. Introducing the spectrum into the  
2 model poses a stronger constraint onto the construction than just utilising the average  
3 pore coordination number. This is due to the fact that totally different spectra could  
4 produce the same average coordination number and the effects of it have been  
5 demonstrated in a number of works (Jivkov et al., 2013; Meyers and Liapis, 1999).

6  
7 Generally speaking there are three ways to construct a PNM representing a porous  
8 medium. The first method is to create a statistically equivalent network using  
9 distributions of basic morphologic parameters, while the second approach is to map a  
10 network structure directly onto a specific porous medium void space. The fundamental  
11 difference between the two methods is that the direct mapping provides a one-to one  
12 spatial correspondence between the porous medium structure and the equivalent  
13 network structure, whereas the other type of network is equivalent only in a statistical  
14 sense to the modelled system. The last method is called the grain-based approach, which  
15 is based on the diagenesis of porous media.

### 17 **3.1 Statistical reconstruction**

18  
19 2D pore space images are routinely available at high resolution. 3D images can be  
20 reconstructed using statistical methods with information obtained by analysing 2D thin  
21 sections. Methods based on a truncated Gaussian random field are often used in  
22 conjunction with the geometrical properties of the original pore space to reconstruct 3D  
23 images (Adler and Thovert, 1998). These geometrical properties include porosity, also  
24 called one-point correlation function, and two-point correlation function measuring the  
25 probability of finding two points separated by a certain distance within the same phase.

26  
27 However, the one and two-point correlations are insufficient to adequately replicate the  
28 topology of the medium (Adler and Thovert, 1998; Ioannidis and Chatzis, 2000; Levitz,  
29 1998; Roberts and Torquato, 1999; Yeong and Torquato, 1998a; Yeong and Torquato,  
30 1998b). Yeong and Torquato (Yeong and Torquato, 1998a; Yeong and Torquato, 1998b)  
31 used a combination of the two-point correlation function and the distribution of linear  
32 path, which is the probability of finding a line segment with certain length in the void

1 space as a descriptor to characterize the pore geometry. In addition, Hilfer (Hilfer, 1991)  
2 introduced local porosity distribution and local percolation probability to improve the  
3 geometrical characterization. Other descriptors, such as pore chord length (the length in  
4 the void between two solid voxels with a given direction) have proved useful in  
5 characterising the structure and generating 3D images (Levitz, 1998; Roberts and  
6 Torquato, 1999). The combination of one- and two-point correlation functions with  
7 these geometrical descriptors improves the reconstruction of connectedness and  
8 predictions of macroscopic properties such as permeability.

9  
10 Despite this, these methods still fail to reproduce the long-range connectivity of the  
11 original pore space. On the other hand, Yeong et al. (Yeong and Torquato, 1998a;  
12 Yeong and Torquato, 1998b) developed a stochastic method based on simulated  
13 annealing, which was later extended by Manwart et. al (Manwart et al., 2000). Their  
14 approach is based on moving pore space voxels around to minimize the objective  
15 function and they obtained the correct porosity. This method should be able to match  
16 not only one- and two- point correlation functions but also multi- point correlation  
17 functions.

18  
19 Okabe and Blunt (Okabe and Blunt, 2004) developed a multi-point statistical method  
20 aiming to reconstruct the 3D volume from thin section images. The approach preserves  
21 the typical void space patterns observed in 2D and consequently preserves the long-  
22 range connectivity. These statistical methods discussed above produce 3D  
23 representation from 2D images of the porous media with similar morphological  
24 statistics.

### 25 26 **3.2 Grain-based model**

27  
28 Bryant and co-workers pioneered the use of geologically realistic networks (Bryant and  
29 Blunt, 1992; Bryant et al., 1993a; Bryant et al., 1993b). Their models are based on  
30 random close packing of equally-sized spheres. They represented diagenesis by swelling  
31 the spheres uniformly and allowing them to overlap. Compaction was modelled by  
32 moving the centres of the spheres closer together in the vertical direction, again

1 allowing the spheres to overlap. Equivalent networks with a coordination number of  
2 four or less were then constructed. Single and multiphase flow was simulated through  
3 the pore space. They were able to predict the absolute and relative permeability,  
4 capillary pressure, electrical and elastic properties of water-wet sand packs, sphere  
5 packs and cemented quartz sandstone. They also reported a trend between permeability  
6 and porosity for Fontainebleu sandstone. This represented a major triumph in pore-scale  
7 modelling, since genuine predictions of transport and flow properties were made for the  
8 first time. They showed that spatial correlations in the pore size distribution were  
9 important for correct predictions: using the same pore size distribution, but assigning it  
10 at random to the throats in the network gave erroneous predictions of permeability  
11 (Bryant et al., 1993a). The main drawback with the work is its limited application—it  
12 could only be applied to media that is predominantly composed of spherical grains of  
13 the same size.

14  
15 The next major advance came with the work of Oren, Bakke and co-workers at Statoil  
16 (Bakke and Oren, 1997; Lerdahl et al., 2000; Oren and Bakke, 2002; Oren et al., 1998).  
17 They developed a reconstruction method, where the packing of spheres of different size  
18 was simulated. The grain size distribution was derived directly from analysis of thin  
19 sections of the rock of interest. Compaction and diagenesis was modelled in a similar  
20 manner to Bryant and co-workers (Bryant et al., 1993a). Clays were also included in the  
21 model. Biswal et al. (Biswal et al., 1999) compared the pore space derived from this  
22 geological reconstruction of Fontainebleau sandstone with an image obtained from  
23 micro tomography. They also studied two stochastic models based on a correlation  
24 function representation. It was shown that the stochastic models differed strongly from  
25 the real sandstone in their connectivity properties. In contrast, the geological  
26 reconstruction gave a good representation of the connectivity of the rock and as a  
27 consequence could accurately predict transport properties (Oren and Bakke, 2002).

28  
29 Oren and co-workers used the geological reconstructions to formulate topologically  
30 equivalent networks through which multiphase flow was simulated (Bakke and Oren,  
31 1997; Oren et al., 1998). They predicted relative permeability for a variety of water-wet  
32 sandstones, showed promising results for a mixed-wet reservoir sample and matched

1 three-phase water-wet data (Lerdahl et al., 2000; Oren and Bakke, 2002). The works of  
2 Pillotti, and Coehlo and co-workers have demonstrated a method to simulate the  
3 deposition of grains of non-spherical shapes, in particular, enabling the reconstruction  
4 technique to be applied more generally (Coelho et al., 1997; Pilotti, 2000).

5  
6 There are three major concerns with the application of reconstruction methods to  
7 reservoir samples. Firstly, the reconstruction algorithm is based on explicit simulation  
8 of the geological processes by which the rock is formed. For many complex systems,  
9 involving microporosity and clays as well as a variety of different sedimentary  
10 processes, this may prove challenging. Furthermore, carbonate systems are not  
11 modelled at all. Statistical reconstruction methods are more general, since they require  
12 only a two-dimensional image of the system, and have been applied successfully to non-  
13 classic rocks. However, their application so far, has been mainly to predict single-phase  
14 flow simulated directly onto the pore-space reconstruction. The second problem,  
15 regardless of the approach, is that characterisation of the pore space requires detailed  
16 thin section analysis that might be unavailable or difficult to obtain. The final issue is  
17 that the appropriate characterization of pore shape and wettability are not fully  
18 understood.

### 20 **3.3 Direct mapping model**

21  
22 Direct mapping from a real sample will yield an irregular lattice (Piri and Blunt, 2005).  
23 Such irregular networks allow for validating physical assumptions for flow simulations  
24 by comparison with 4D imaging of mass transport. 4D (3D + time) imaging  
25 methodology enables visualization and quantitative assessment of dynamic pore scale  
26 processes in real time over variable experimental durations. More details can be found  
27 at <http://www.solid-earth-discuss.net/se-2016-40>. Based on 3D images, the following  
28 approaches have been used to construct irregular pore network models.

#### 30 3.2.1 Medial axis algorithm

1 The medial axis based methods transform the pore space images into a medial axis that  
2 was the reduced representation of the pore space acting as a topological skeleton. The  
3 topological skeleton is constructed roughly along the middle of the pore channels either  
4 by a thinning algorithm (Baldwin et al., 1996; Liang et al., 1998) or a pore-space  
5 burning algorithm (Lindquist et al., 1996). The algorithms developed by Lindquist et al.  
6 (Lindquist et al., 2000) have been primarily applied to consolidated systems but it is  
7 unknown whether they are applicable to unconsolidated porous media with higher  
8 porosity. Al-Raoush et al. (Al-Raoush et al., 2003) developed algorithms which can be  
9 applied to unconsolidated porous media and demonstrated their application on a variety  
10 of unconsolidated porous media systems and the impacts of grain sizes, REV, and  
11 image resolution (Al-Raoush and Willson, 2005). The pore throats are decided by local  
12 minima along the branches whereas the pore bodies are determined at the nodes, which  
13 verify pore space partitioning (Jiang et al., 2007; Lindquist et al., 1996; Prodanović et  
14 al., 2006).

15

16 The medial axis mathematically preserves the topology of the pore space; it is difficult,  
17 however, to identify pores unambiguously. Furthermore, pores normally encompass  
18 more than one junction of the medial axis; therefore, various merging algorithms have  
19 to be developed to trim the skeleton and fuse the junctions together while avoiding  
20 unrealistically high coordination numbers (Jiang et al., 2007; Shin et al., 2005). The  
21 choice of threshold value for throat quality can be problematic without being examined  
22 by real flow simulations. In conclusion, medial axis algorithms readily capture the  
23 interconnectivity of the pore spaces but encounter the problem in identifying pores.

24

### 25 3.2.2 Maximal ball algorithm

26

27 The maximal ball algorithm (Al-Kharusi and Blunt, 2007; Silin and Patzek, 2006) finds  
28 the largest inscribed spheres centred on each voxel of the image that just touch the grain  
29 or the boundary. Then those spheres, which are included in other spheres, are removed,  
30 while the rest are called maximal balls. The largest maximal balls usually identify pores,  
31 which are connected by smaller balls between them (these balls are called throats).  
32 Maximal balls were first used by Silin et al. (Silin and Patzek, 2006) to find the

1 dimensionless capillary pressure in drainage rather than to extract a pore network. The  
2 method was then adopted and developed by Al-Kharusi and Blunt (Al-Kharusi and  
3 Blunt, 2007). A more comprehensive set of criteria was set to determine the maximal  
4 ball hierarchy including sphere clusters to handle equally sized balls. However, the  
5 algorithms of Al-Kharusi and Blunt use a tremendous amount of computer memory and  
6 time and consequently were limited to relatively small systems containing fewer than a  
7 thousand pores. Moreover, their method tended to form pores with very high  
8 coordination numbers. To overcome this issue, a two-step searching algorithm was  
9 developed by Hu dong et al. (Dong and Blunt, 2009) based on Al-Kharusi and Blunt's  
10 algorithm. The nearest solid was found to define a void bass instead of growing a ball  
11 layer by layer. This algorithm invented a clustering process to define pores and throats  
12 by affiliating the maximal balls into family trees according to their size and rank (Dong  
13 and Blunt, 2009). This method clearly identified the larger pores, but tended to indentify  
14 a cascade of smaller voids, which have sizes less than the image resolution.

15

16 One of the problems in network generation and modelling is the lack of a specific  
17 definition for what constitutes pores and pore throats in real materials with complicated  
18 pore geometries. Another problem is how the definition of pore morphology affects  
19 network topology and discretization. Consequently, multiple network structures can be  
20 created for the same material or 3D data set and there is no straightforward way to  
21 define whether one network is more physically representative than another. Vogel  
22 (Vogel, 2000) has demonstrated that different lattice-based topologies have similar  
23 water retention curves. Inversely, Ams et al. (AMS et al., 2004) have demonstrated that  
24 different network topology induce different relative permeability.

25

26 The effects of pore density (number of pores per unit volume) on transport in porous  
27 media have been studied by Bhattad et al (Bhattad et al., 2011). The large variations in  
28 pore density are the result of two factors: different methods for seeding the search for  
29 pores (i.e. defined as maximal inscribed spheres) and different settings in the merging  
30 criteria (that merges overlapping inscribed spheres to created single pores). Generally,  
31 the fast algorithms create low-density networks with little or no overlap in inscribed  
32 pores and therefore, can also generate longer pore–throats. More complete pore searches

1 are slow and result in higher pore densities and shorter pore–throats. The pore density  
2 affects secondary parameters, such as pore-size distribution and pore interconnectivity.  
3 However, the relationship is not always proportional or obvious. The most important  
4 results have shown that single-phase permeability is relative insensitive to pore density,  
5 while capillary pressure curves for quasi-static drainage are moderately sensitive to  
6 network structure (Bhattad et al., 2011)

### 8 **3.4 Regular network model**

9  
10 Irregular PNM are sample-specific and potentially not statistically representative. Direct  
11 construction of irregular network is impossible (especially for micro- and meso-porous  
12 materials) in the absence of data for throat locations and sizes, which cannot be  
13 observed by current imaging techniques. A regular PNM constructed within a larger  
14 volume allows for capturing statistics from a number of imaged samples, i.e. improved  
15 statistical correspondence, and for calculating transport at distances closer to the  
16 engineering length scale.

17  
18 Early three-dimensional network models are usually based on cubic lattice with a  
19 constant coordination number of six, Fig. 1(a) (Ioannidis and Chatzis, 1993b; Reeves  
20 and Celia, 1996). However, in actual porous media, the connectivity is distributed and  
21 can have coordination number greater than six (Dong and Blunt, 2009; Jivkov et al.,  
22 2013; Kwiecien et al., 1990). Therefore models with 26 pore coordination number have  
23 been proposed, Fig. 1(b) (Raouf and Hassanizadeh, 2010a). This does not appear to be  
24 physically realistic, however, because large numbers of throats intersect at points that  
25 are not pores. A pore network construction based on the Kelvin solid has been recently  
26 proposed and applied to permeability and diffusion analyses of porous media, Fig. 1(c)  
27 (Jivkov et al., 2013; Xiong et al., 2014). This is based on truncated octahedral cells  
28 providing variable pore coordination dependent on the allocation of pores and throats in  
29 the cell, with maximum coordination of 14. Another application of a non-cubic lattice  
30 support for pore-network construction uses rhombic dodecahedron as a unit cell, Fig.  
31 1(d) (Vogel and Roth, 2001). This offers a maximum pore coordination of 12 with  
32 throats of equal lengths, i.e. sufficiently large physically admissible coordination.

1 However, this cell is less representative for the volume around a pore than the truncated  
2 octahedral cell.

3

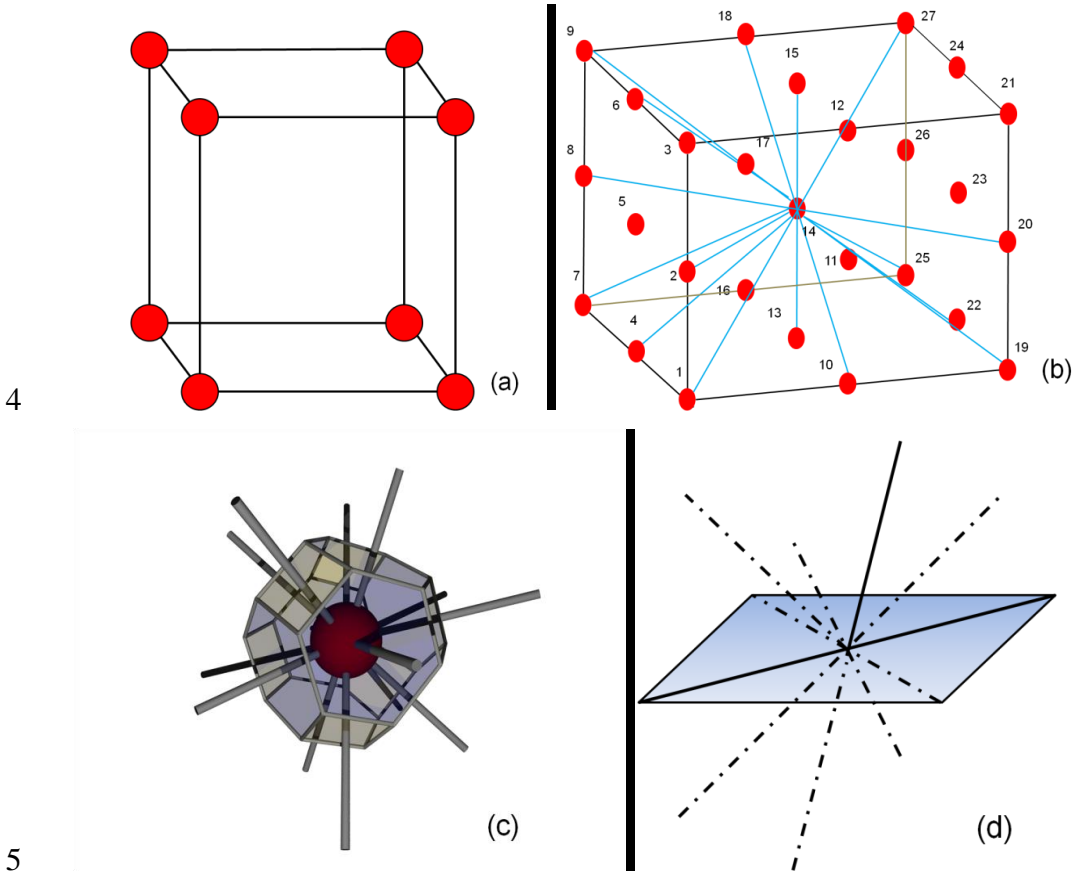


Fig. 1 Unit cell shapes: (a) cubic lattice with a constant coordination number of six (Ioannidis and Chatzis, 1993b; Reeves and Celia, 1996); (b) cubic lattice with 26 pore coordination number (Raouf and Hassanizadeh, 2010a);(c) truncated octahedron (Jivkov et al., 2013; Xiong et al., 2014); (d) rhombic dodecahedron (Vogel and Roth, 2001).

10

11 Historically, pores were related to the sites while pore throats were related to the bonds  
12 of regular PNM (Dillard and Blunt, 2000; Meyers et al., 2001; Wilkinson and  
13 Willemsen, 1983). If such correspondence is to be statistically representative of the  
14 material modelled, sufficiently rich experimental information is required. This  
15 information includes shape and size distribution of pores and throats, as well as the pore  
16 coordination spectrum, i.e. percentages of pores coordinated by different numbers of  
17 throats (Gao et al., 2012; Jivkov et al., 2013). These can be obtained in structures with  
18 distinguishable pores and pore throats.



1  
2 For porous media with macro-porosity, typically above 100 nm such as sandstone and  
3 limestone, the throat and pore sizes distribution can be resolved as well as the  
4 coordination spectra and the average coordination numbers can be calculated (Al-  
5 Raoush and Willson, 2005; Dong and Blunt, 2009). In such cases, topologically  
6 representative networks can be constructed by a system of pores and throats connecting  
7 all neighbouring pores, and subsequent elimination of throats to achieve the topological  
8 constraints. This has been illustrated for average coordination number in simple bases,  
9 such as cubic lattice (Raouf and Hassanizadeh, 2010a), as well as for full coordination  
10 spectra in a bi-regular lattice (Jivkov et al., 2013).

11  
12 However, for micro- and meso-porosity, e.g. below 100 nm, the pore size distribution  
13 can usually be determined, but the resolution of the experimental techniques is not  
14 sufficient to segment all the throats and calculate their sizes. For such cases, different  
15 approaches to pore network construction are required. One possibility is to assume full  
16 connectivity between neighbouring pores in a selected lattice, but control the diffusivity  
17 of the throats through the sizes of the connected pores and the size of the solute  
18 molecules (Xiong et al., 2014). This construction leads to a model length scale dictated  
19 by the prescribed total porosity and the assumption that pores are located at each lattice  
20 site. The approach was shown to provide insights into the effects of the structure on  
21 diffusivity and the results correlated well with experimentally measured diffusion  
22 coefficients (Xiong et al., 2014). This approach, however, is not sufficient to explain the  
23 variability in reported experimental measurements of diffusion coefficients.

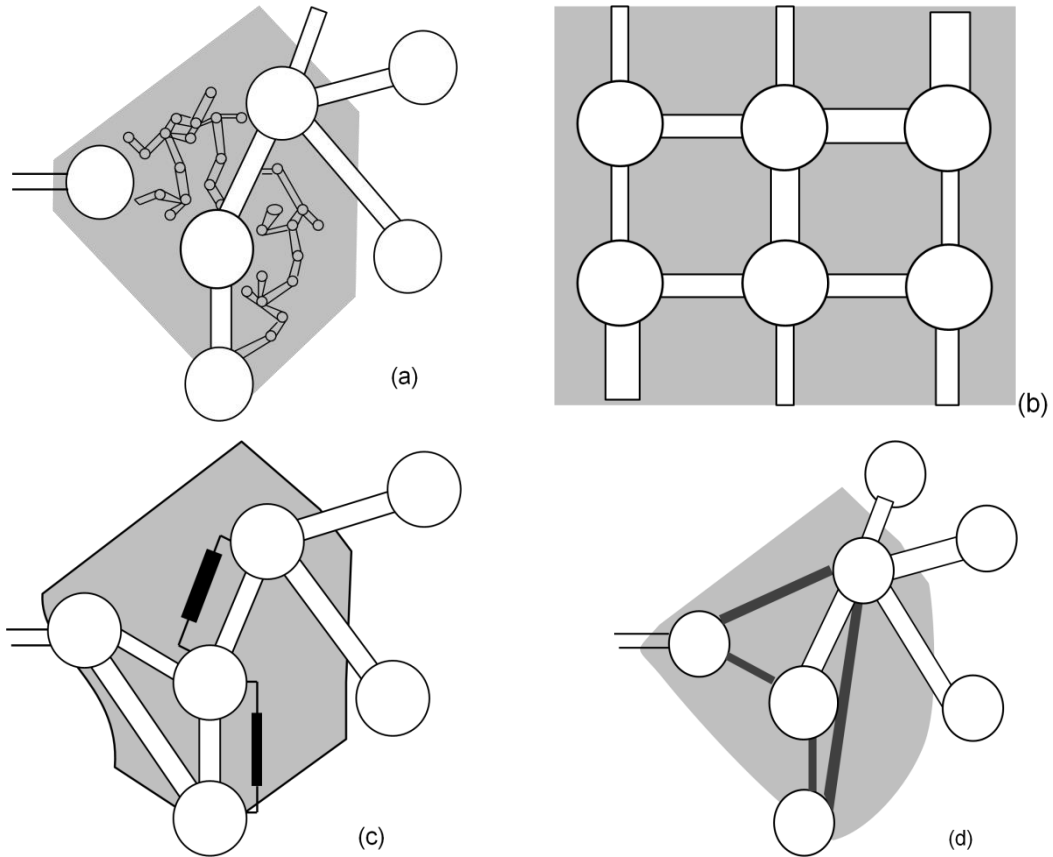
24  
25 Clearly, the microstructure information used for the network construction is derived  
26 from samples, which are different from the ones used for measurements of diffusion  
27 coefficients. It is plausible, however, to assume that the statistical part of this  
28 information, namely the distribution of pore sizes, is not vastly different between  
29 samples of the same medium. This implies that there is an effect of an additional  
30 geometrical parameter on the measured coefficients. It could be possible that a network  
31 length scale that provides a constraint to the model rather than being determined from  
32 total porosity and location of pores in all lattice sites (Jivkov and Xiong, 2014).

1  
2  
3  
4  
5  
6  
7  
8  
9  
10  
11  
12  
13  
14  
15  
16  
17  
18  
19  
20  
21  
22  
23  
24  
25  
26  
27  
28  
29  
30  
31

The two approaches that tackle incomplete pore space information, namely predefined connectivity for calculable length scale (Xiong et al., 2014), and undetermined length scale for realistic connectivity (Jivkov and Xiong, 2014), suffer from the lack of an additional constraint. This cannot be found from the pore space information and requires the consideration of the solid phase structure, e.g. the shape and size distribution of mineral grains. A methodology for incorporating the structure of the solid phase was then proposed which improves substantially the realism of the constructed pore network, both in terms of geometry and topology (Xiong and Jivkov, 2015). The proposed methodology is conceptually different from previous works and it has the added benefit of constructing a PNM which can be paired directly to lattice models of the solid phase, developed for analysis of damage evolution via micro-cracking (Jivkov et al., 2012; Zhang and Jivkov, 2014). The approach is conceptually similar to the dual models of pore spaces introduced by Glantz et al. (Glantz and Hilpert, 2007; Glantz and Hilpert, 2008). This facilitates mechanistic investigations of combined mechanical-thermal-chemical-biological effects on diffusivity.

### 3.5 Two-scale pore network models

Despite the advances of pore scale modelling, the simulation of transport properties in heterogeneous rocks still remains an open issue due to the very broad pore size distributions in some porous media. Such examples could be of considerable scientific and economic importance including many types of carbonates, clay-rich sandstones and clays. For example, carbonate reservoirs or tight gas sandstones are very important for hydrocarbon extraction and CO<sub>2</sub> sequestration. The failure of simulating most classical empirical relations (e.g. the Brooks–Corey parameterization of relative permeability and Archie’s law for electrical behaviour) in these rocks due to the interaction of micro- and macro-porosity in turn has promoted the development of modelling methods where multiple pore scales are coupled (Mehmani and Prodanović, 2014). A short overview of existing two-scale pore network models is presented here and illustrated in Fig. 2.



1

2 Fig. 2. Schematic depiction of existing DPNM methods. In all figures, light grey  
 3 represents a zone of microporosity. (a) a model with individual micropores (Jiang et al.,  
 4 2013; Prodanović et al., 2015). (b) a lattice-based model with upscaled microporosity  
 5 properties (Bekri et al., 2005). (c) a model which takes upscaled microporosity in  
 6 parallel with macro-throats (dark grey) into account (Bauer et al., 2012). (d) a model  
 7 with connectivity added by the (upscaled) microporosity (Bultreys et al., 2015).

8

9 Jiang et al. (Jiang et al., 2013) developed a methodology to integrate networks extracted  
 10 from images at distinct length scales. The pore network model was generated at each  
 11 scale and then was integrated into a single two-scale network by characterizing the  
 12 cross-scale connection structure between the two networks. The shortcoming of this  
 13 method is that it is computationally costly due to the number of network elements  
 14 (Bultreys et al., 2015). Recognizing the computational problems when single micro-  
 15 pores are taken into account, Mehmani and Prodanović (Mehmani and Prodanović,  
 16 2014) proposed a two-scale pore network by the use of packing algorithms. The macro-  
 17 network is constructed by Delaunay tessellation of the grain centres. Micro-porous

1 networks are generated by downscaling existing networks extracted from macro-pores.  
2 This approach was capable of investigating fundamental two-phase flow properties of  
3 multi-scale porous media and micro-porosity was able to act in series (intergranular or  
4 pore-filling micro-porosity) and in parallel (intra-granular or dissolution micro-porosity)  
5 to the macro-pores. However, in the construction process, distorted pores were produced  
6 when many small grains touched a large grain. A parameter, the ratio of the macro to  
7 micro length scale, needs to be determined for micro-porous regions from the  
8 measurements, which may be difficult to perform. Bultreys et al. (Bultreys et al., 2015)  
9 developed a workflow to integrate networks of macro-pores and micro-porous regions  
10 extracted from micro-CT images. This methodology allowed micro-porosity to act both  
11 in parallel and in series with the macro-pore network. However, a representative  
12 network for the micro-porosity is necessary. In addition, the pore networks from Jiang  
13 et al. (Jiang et al., 2013) and Boultry et al. (Bultreys et al., 2015) were based on  
14 experimental data from micro-CT images which did not take into account the micro-  
15 pores that cannot be resolved by micro-CT. As the truncated cone shape is used to  
16 connect two neighbouring macro-pores, the tortuosity of the connection and geometric  
17 details about the bulk of the micro-porous cluster are neglected, which can lead to  
18 erroneous local conductivities.

19

## 20 **4. Applications**

21 Pore network models have been used to explore reactive transport processes, such as:  
22 adsorption (Acharya et al., 2005; Raouf et al., 2013), dissolution/precipitation (Kang et  
23 al., 2010; Knutson et al., 2001; Mehmani et al., 2012; Varloteaux et al., 2013; Zhou et  
24 al., 2000), and biomass growth (Dupin et al., 2001a; Gharasoo et al., 2012; Rosenzweig  
25 et al., 2013). In this section, we review some representative applications of the PNM in  
26 these areas.

27

### 28 **4.1 Adsorption**

29

30 PNM has been widely used to study adsorption in porous media which finds its  
31 relevance in many areas of science and engineering including radioactive waste disposal

(Xiong et al., 2015a; Xiong et al., 2014) and chromatographic separation processes (Câmara and Silva Neto, 2009; Meyers and Liapis, 1999).

There are two principal ways to simulate adsorption in PNM. The first one entails decoupling of adsorption and transport into two separate processes by the use of parameters associated with each process calculated separately. Firstly, the convection-diffusion problem is solved to obtain the concentration and flow field. This is governed by the following equations:

$$q_{ij} = \frac{A_{ij}^2 G_{ij}}{\mu l_{ij}} (p_i - p_j) \quad (1)$$

$$V_{ij} \frac{dc_{ij}}{dt} = q_{ij} (c_i - c_j) + D_{ij} A_{ij} \frac{c_i - c_j}{l_{ij}} \quad (2)$$

where Eq. (1) is the Hagen- Poiseuille law, appropriate for describing flow in pores (Jacob, 1972) and valid for laminar flow; and Eq. (2) is the classical convection-diffusion law. The equations are written for transport through a throat connecting pores  $i$  and  $j$ , with length  $l_{ij}$  [L], and cross section area  $A_{ij}$  [L<sup>2</sup>]. In Eq. (1)  $q_{ij}$  [L<sup>3</sup>T<sup>-1</sup>] is the total volumetric flow rate through the throat,  $p_i$  and  $p_j$  [ML<sup>-1</sup>T<sup>-2</sup>] are pressures at pores  $i$  and  $j$ , respectively,  $\mu$  [ML<sup>-1</sup>T<sup>-1</sup>] is the dynamic viscosity, and  $G_{ij}$  is a cross-section shape coefficient: for circular, equilateral triangle and square tube,  $G_{ij}$  is 0.5, 0.6 and 0.5623 respectively (Patzek and Silin, 2001). In Eq. (2)  $V_{ij}$  [L<sup>3</sup>] is the throat volume,  $c_i$  and  $c_j$  [ML<sup>-3</sup>] are concentrations at pores  $i$  and  $j$ , respectively, and  $D_{ij}$  [L<sup>2</sup>T<sup>-1</sup>] is the throat diffusivity.

Then, a sorption isotherm, which is assumed to belong to some class of parameterized functions (Langmuir, Freundlich, Henry, etc.) with few tuning parameters, is used to describe the adsorption of species onto the walls. A coarse grained mathematical formula containing the sorption isotherm is used to reflect the effects of sorption on the change of pore sizes. For example, the adsorbate obstruction can be simulated by reducing the throats radii as a function of the concentration of the moving species (Meyers and Liapis, 1999; Xiong et al., 2015a; Xiong et al., 2014)

$$t^2 - 2tR + 8\theta Rr_M / 3 = 0 \quad (3)$$

1 where  $t$  is the thickness of the adsorbed layer,  $R$  is the throat radius,  $r_M$  is the radius of  
2 the diffusing species, and  $\theta$  is the adsorption isotherm (e.g.  $\theta_{ij} = k_{d,ij}c_{ij}$ ,  $\theta_{ij} = ac_{ij}^b$ ). Thus,  
3 the radius of a throat after adsorption at given concentration,  $C_A$ , and hence radius after  
4 adsorption, becomes  $R^* = R - t$ . Thus, the sorption is accounted for by modifying the  
5 pore geometries according to the changed pore sizes. This procedure is iterated until  
6 reaching a certain criteria of interest. Using this method, various types of adsorption  
7 reactions can be studied, including linear equilibrium, nonlinear equilibrium (Meyers  
8 and Liapis, 1999; Xiong et al., 2014) and heterogeneous adsorption in which the  
9 adsorption parameters are spatially varying (Xiong et al., 2015a).

10  
11 Sorption isotherms in the published literature, however, are determined from bulk  
12 measurements and may not be appropriate for occluded regions within the pore space.  
13 Adsorption takes place at the water–solid interface and is thus controlled by solute  
14 concentration in the fluid next to the solid grain in individual pores. The concentration  
15 near the solid surface is different from the average concentration within the pore due to  
16 the development of concentration gradients within the pore space. Simulations with  
17 pore network models are usually based on the average concentration in individual pore  
18 throats. An alternative way is to simulate the adsorption in each pore element and then  
19 scale it up to the whole pore network. This has been demonstrated by Raouf and  
20 Hassanizadeh (Raouf and Hassanizadeh, 2010b). They have performed pore-scale  
21 simulations for a wide range of local-scale distribution coefficients and Peclet numbers.  
22 These have provided relationships between the upscaled parameters and underlying  
23 pore-scale parameters. Such relations are useful for upscaling by means of a pore-  
24 network model. Raouf and Hassanizadeh have shown also that even if there were  
25 equilibrium adsorption at the pore wall (i.e. at the grain surface), one might need to  
26 employ a kinetic description at larger scales. They have also shown this kinetic  
27 behaviour through a volume averaging method, yielding very similar results for the  
28 upscaled kinetic parameters. From upscaling, they have found a negligible dependency  
29 of effective adsorption rate coefficients on pore water velocity. This finding is in  
30 agreement with Zhang et al. (Zhang et al., 2008) who has observed that upscaled  
31 sorption parameters are independent of pore-water velocity. The findings, however,  
32 contradict some experimental results, where kinetic adsorption–desorption coefficients

1 have been shown to depend on velocity (Akhratanakul et al., 1983; Brusseau, 1992;  
2 Maraqa et al., 1999; Pang et al., 2002).

3

4 The second principal method for simulating adsorption in PNM is by solving the  
5 advection-diffusion-sorption equation directly. The adsorption reactions include linear  
6 equilibrium (Raouf et al., 2013) and nonlinear equilibrium (Acharya et al., 2005; Xiong  
7 et al., 2015b). The equation can be expressed as

$$8 \quad V_{ij} \frac{dc_{ij}}{dt} = V_{ij} u_{ij} \frac{c_i - c_j}{l_{ij}} + F_{ij} - S_{ij} \frac{ds_{ij}}{dt} \quad (4)$$

9 where  $V_{ij} u_{ij} \frac{c_i - c_j}{l_{ij}}$  is the advection term which represents the effects of velocity  $u_{ij}$  on

10 particle transport,  $F_{ij} = A_{ij} D_{ij} \frac{d^2 c_{ij}}{dx^2}$  is the diffusive term,  $s_{ij} = s_{ij}(c_{ij})$  [ML<sup>-2</sup>] is mass  
11 adsorbed per unit area of throat wall,  $S_{ij}$  [L<sup>2</sup>] is the throat surface area.

12

## 13 **4.2 Dissolution and precipitation**

14

15 Modelling of dissolution/precipitation is of high interest to applications such as CO<sub>2</sub>  
16 geological storage, enhanced oil recovery and chemical degradation of the cement. For  
17 example, CO<sub>2</sub> storage is one possible method to reduce atmospheric emissions of CO<sub>2</sub>,  
18 and hence mitigates climate change. Some CO<sub>2</sub> may dissolve in the resident brine and  
19 generates a weak acid after injection into the low-permeability caprock. The acidic CO<sub>2</sub>-  
20 rich brine reacts with the host rock to produce solid carbonate which leads to  
21 precipitation process (Blunt et al., 2013). In enhanced oil recovery, strong acid has been  
22 injected near the well to dissolve the host rock and increase the reservoir permeability  
23 (Algive et al., 2010). Accurately computing dissolution and precipitation processes  
24 involve the development of advection, diffusion and reaction equations. In addition, for  
25 better estimation of the abovementioned process the following also need to be  
26 accounted for: the heterogeneities in the porous media (e.g. porosity, mineralogical and  
27 chemical compositions), geometrical changes (i.e. pore and throat size changes),  
28 topological changes (i.e. increase/decrease pore to pore connection) and the chemical  
29 gradient field inside pores. This is due to the fact that mineral dissolution and

1 precipitation reactions alter the geometry and topology of the porous media (Crandell et  
2 al., 2012).  
3  
4 Li et al. (Li et al., 2006) used a pore-scale network model to simulate reaction of  
5 kaolinite and anorthite during carbon sequestration. The processes of diffusion,  
6 advection, aqueous reactions, dissolution and precipitation were simulated in individual  
7 pores. The information was then summarised and averaged over the network to obtain  
8 descriptions of processes at the continuum scale. As previously observed, they showed  
9 qualitatively that in situ reaction rates were significantly different from values found in  
10 batch lab reactors. Their network models, however, were 3D regular lattices and not  
11 physically representative of the real media, which made quantitative analysis  
12 challenging. Li et al. (Li et al., 2007) further investigated the influence of the spatial  
13 distribution of mineral species using hypothetical networks, while Kim et al. (Kim et al.,  
14 2011a) used network models mapped from X-ray computed tomography(XCMT) of real  
15 sandstones. They were able to determine the initial concentrations of minerals in the  
16 porous medium from the XCMT images, which allowed for more predictive modelling.  
17 Kim et al. (Kim et al., 2011b) studied the relationship of reaction rates with kinetic rate  
18 and bulk flow rate based on previous work (Li et al., 2007; Li et al., 2006). The  
19 reaction rates were found dependent on flow rates with an approximately power law  
20 relationship. They noted that their models were limited by the size of the network model.  
21 Notably, the effects of decreased throat conductivity as a result of precipitation were not  
22 accounted for in their work. Thus the physical change in porosity is lacking in the  
23 network flow model due to surface minerals dissolving or precipitating. These models,  
24 therefore, do not capture the important topological changes that reactions produce and  
25 the impact that such changes may induce on upscaled reaction rates. Algorithms for  
26 incorporating physical change, due to dissolution and precipitation, need to be included  
27 in the models. Based on these limitations, Kim et al. (Kim and Lindquist, 2013) further  
28 extended the work to consider geometric changes (e.g. pore volume and reactive surface  
29 area) and topological changes, which opened new connections between porosity  
30 features. When geometrical changes are included, the steady state, core-scale reaction  
31 rates could not be directly used as input into larger-scale simulations, as reactions are  
32 time dependent. The Nernst-Planck (N-P) term in the governing transport equations,



1 which ensures the electrical neutrality when species of different charges diffuse at  
2 different rates, was also taken into account. The agreement between simulations with  
3 and without the N-P term improved as the flow rate decreased. In these studies,  
4 reactions far from equilibrium, such as anorthite reaction, and reactions close to  
5 equilibrium conditions, such as the kaolinite reaction, were considered.

6  
7 Algive et al. (Algive et al., 2010) used a pore-scale model to simulate reactive transport  
8 which caused precipitation in pores. The reactive transport and structural modifications  
9 were treated separately and updated step by step. The reactive transport was solved in  
10 each element of the pore network. The mean concentration in each pore was used to  
11 determine the effective parameters of the macroscopic reactive transport equation. The  
12 different pore geometries were also considered for reactive transport by using random  
13 walk techniques. Then the reactive transport equation was solved analytically between  
14 the nodes of the regular lattice network for the asymptotic regime and computed the  
15 node concentration by a matrix inversion. Moreover, the system was based on the  
16 assumption that it had nearly reached chemical equilibrium and mainly focused on  
17 regular or periodic networks in one or two dimensions or systems, where pore-to-pore  
18 heterogeneity was not taken into account.

19  
20 Algive et al. (2012) developed a methodology to use a reactive pore network model to  
21 extract upscaling factors to tie the pore-scale effects of reactive transport to the core-  
22 scale values of permeability and porosity. Their work simplified the geochemistry and  
23 transport by incorporating most geochemical dynamics and transport into dimensionless  
24 variables and in doing so prevented a full description of the different physical and  
25 chemical parameters. Mehmani et al. (Mehmani et al., 2012) developed a novel  
26 approach that coupled several pore-scale models using mortar coupling domain  
27 decomposition to study the evolution of precipitation-induced cementation of calcite.  
28 They were able to study large changes in permeability and porosity by coupling of 64  
29 pore-scale models (1 mm × 1 mm × 1 mm each) but with a limited description of the  
30 chemistry represented by two main parameters, the Damkohler number ( $D_a$ ) and an  
31 “*alpha*” parameter which described the deviation from equilibrium of the precipitation  
32 reaction. Nogues et al. (Nogues et al., 2013) simulated carbonic acid-driven reactions in

1 a 3-D network of pores to predict the changes in permeability and porosity at continuum  
2 scale. The pore network structure was based on a statistical characterization of a  
3 synthetic microcomputed-tomography image of an oolitic dolostone. Only physical  
4 heterogeneities were considered in comparison to the work done by Kim et al. (Kim et  
5 al., 2013). To account for the changes caused by dissolution and precipitation, a  
6 mathematical construct was developed to modify the pore-pore conductivities by  
7 relating these changes to changes in pore volumes. It is important to note that while the  
8 surface area fractions assigned to different minerals do change, the model does not  
9 change the total surface area. Because the reactions are modelled at equilibrium, the  
10 reaction rate is independent of surface area. Thus the simulation results are negligibly  
11 affected in this situation. This model analysed the effects of different chemical, flow  
12 and mixing conditions on permeability.

13

14 Raoof et al. (Raoof et al., 2013; Raoof et al., 2012) employed a coupled Complex Pore  
15 Network Model (CPNM) and Biogeochemical Reaction Network Simulator (BRNS) to  
16 solve reactive transport by pore networks. CPNM reproduced the microstructure of real  
17 porous media and calculated solute concentration values for both pore bodies and pore  
18 throats within the pore network. BRNS (Regnier et al., 2002) was responsible for  
19 handling a comprehensive suite of multi-component complexation, mineral precipitation  
20 and dissolution reactions, as well as reaction networks characterized by multiple kinetic  
21 pathways. The evolution of porosity and permeability was discussed in this work as  
22 well. In BRNS the processes of dissolution/precipitation were simulated by changes of  
23 radius of pores and throats, while the effects of opening/clogging pores/throats were not  
24 considered.

25

26 All modelling approaches mentioned above involve the assumption that mass transfer  
27 within the pore is not limited, and that the regular geometric solid-fluid interface and the  
28 aqueous concentrations are spatially uniform within a pore. Based on that, the pore  
29 network models do not resolve chemical gradients within pores and also for each single  
30 pore the average values for physical/chemical properties were used. The accuracy of  
31 this assumption in computing reactive flow requires further investigation.

32

### 1 **4.3 Biomass growth**

2  
3 Biomass growth within porous media is of particular interest in a variety of industrial  
4 scenarios such as microbial enhanced oil recovery (Ezeuko et al., 2011), bioremediation  
5 of contaminated soil and water (Cunningham et al., 1991) and nuclear waste disposal.  
6 As the mass of the microorganisms grows, hydrodynamic properties of porous media  
7 change (Rolland du Roscoat et al., 2014; Stewart and Scott Fogler, 2002; Taylor and  
8 Jaffé 1990). The relevance of PNM to biofilm growth modelling comes from the fact  
9 that the biomass is not homogeneously dispersed within the porous media and hence  
10 continuum models fail to adequately represent this pore-scale phenomena and its effect  
11 on the macroscopic properties of the media.

12  
13 The morphology of biomass growth in porous media depends strongly on the structure  
14 of the porous medium, bacteria species and the prevailing hydrodynamic and nutritional  
15 conditions. Wimpenny et al presented a good review of the factors affecting biofilm  
16 formation (Wimpenny et al., 2000). Three principal morphologies have been reported in  
17 the literature: flat and uniformly thick biofilms, mushroom-shaped structures and  
18 streamers (Stoodley et al., 1999). Only the first two, however, have significant  
19 relevance to porous media since streamers generally occur at turbulent flow conditions.  
20 The most commonly modelled growth mode is a continuous layer on the surface of the  
21 soil grains (Suchomel et al., 1998). Sometimes, however, the biomass does not cover  
22 the entire surface of the soil grains, and thus microcolonies, i.e., a patchy biofilm,  
23 develop (Molz et al., 1986). In other cases, biomass grows in pores in the form of  
24 aggregates (Vandevivere and Baveye, 1992). When fungal growth occurs, mycelia can  
25 develop throughout the entire pore volume and envelop several soil grains (Dupin and  
26 McCarty, 2000). These forms of biomass growth can occur simultaneously (Dupin and  
27 McCarty, 2000). Biofilm morphology is important because it results in different  
28 clogging mechanisms. Rittmann (Rittmann, 1993) noted that the difference between flat  
29 biofilms, and aggregate growth is crucial to model permeability reduction. It takes less  
30 biomass to plug a pore if it forms aggregates as opposed to continuous biofilms.  
31 Therefore, mushroom-shaped colonies have the potential to generate larger permeability  
32 reductions in comparison to the uniform biofilm morphology (Thullner, 2010).

1  
2 The development of robust methods to engineer biofilms in porous media requires  
3 predictive mathematical models capable of determining the evolution of biofilms under  
4 different flow conditions. However, reported studies of biofilm evolution in micro  
5 models have revealed that the structural complexity of biofilms entrapped in a complex  
6 pore space makes accurate modelling difficult (Dupin and McCarty, 2000; Kim and  
7 Fogler, 2000). Several pore level models for biofilm growth under flow conditions have  
8 been developed by adopting different approaches. They include lattice Boltzmann-based  
9 models (Pintelon et al., 2009; Pintelon et al., 2012), bacterial cell level individual-based  
10 models (Kreft et al., 2001; Picioreanu et al., 2004), and Pore Network Models (PNMs)  
11 (Kim and Fogler, 2000; Stewart and Kim, 2004; Suchomel et al., 1998; Thullner and  
12 Baveye, 2008). Ezeuko et al. modelled biofilm evolution in porous media using a new  
13 PNM that includes hydrodynamics and nutrient transport based on coupling of  
14 advective transport with Fickian diffusion, and a reaction term to account for nutrient  
15 consumption. Specifically, the PNM is used to examine the influence of biofilm  
16 formation on the hydraulic properties of porous media. In PNM models, pore  
17 geometries can range from a simple circular cylinder through to complicated voxel-by-  
18 voxel pore reconstructions from thin sections or micro-tomographical data. The PNM  
19 approach facilitates simulations of important processes by adopting simplified but  
20 realistic pore geometries while allowing implementations of other pore level physics  
21 and kinetics relevant to the process of interest (Ezeuko et al., 2011).

22  
23 Or and Tuller (Or and Tuller, 2000) used the classic capillary tube model to represent  
24 the soil pores (i.e., the pores are simulated as a bundle of capillary tubes of different  
25 diameters) and studied flow in unsaturated fractured porous media. The analysis showed  
26 that the biofilm spatial distribution within the pore space has a significant effect on the  
27 hydraulic properties of the soil. Although the capillary model is widely used and is easy  
28 to obtain, it has a few shortcomings, primarily the over simplistic assumption regarding  
29 the binary nature of the pores (i.e., each pore is either completely water-filled or  
30 completely empty under a prescribed matric head). Moreover, the lack of pores  
31 connectivity and the unrealistic cylindrical geometry of the capillaries further reduce the  
32 model efficiency in determining soil hydraulic properties (Or and Tuller, 2000). Or and

1 Tuller (Or and Tuller, 2000) suggested to model the soil-pores by using channels having  
2 a triangular cross-section. The channels can be either water-filled (for saturated flow) or  
3 partially-filled (for unsaturated flow), where the water-filled fraction is related to the  
4 matric head through the curvature of the water surface. The lack of pore connectivity  
5 can be especially significant when dealing with biofilms. Thullner et al. (Thullner et al.,  
6 2004; Thullner et al., 2002) showed that under saturated conditions, modelling the pores  
7 as one-dimensional capillary tubes could not reproduce connectivity-related effects.  
8 These effects, such as flow bypasses generated from preferential biofilm growth, were  
9 demonstrated in experiments and were successfully reproduced using pore-network  
10 models. Rosenzweig et al. extended Or and Tuller's (Or and Tuller, 2000) concept and  
11 propose a framework in which the soil pores are simulated as a network of channels  
12 having a triangular cross-section. The representation of the soil pores by a network of  
13 triangular channels is superior to the capillary model in two aspects. It eliminates the  
14 binary (full/empty) behaviour and takes into account inter-pore connectivity.  
15 Furthermore, it provides basis on simulating the combined water flow, solute transport  
16 and biofilm growth under variably saturated conditions (Rosenzweig et al., 2013).

17

18 The coupled water flow, substrate transport, and biofilm growth under saturated  
19 conditions has been studied by several researchers by using pore network models  
20 (Dupin et al., 2001b; Kim and Fogler, 2000; Suchomel et al., 1998; Thullner and  
21 Baveye, 2008; Thullner et al., 2002). To study the effects of biofilm on porous media,  
22 the pore network models were built either of lattices of cylindrical tubes (Kim and  
23 Fogler, 2000; Suchomel et al., 1998; Thullner and Baveye, 2008), or two-dimensional  
24 channels (Dupin et al., 2001b). The biofilm was modelled as either a continuous layer  
25 coating pore walls (Suchomel et al., 1998; Thullner and Baveye, 2008; Thullner et al.,  
26 2002) or as isolated microcolonies (Dupin et al., 2001b; Thullner et al., 2002). As  
27 biomass growth depends on the environmental conditions and the type of bacteria, it is  
28 problematic to represent this accumulation appropriately in terms of its effect on  
29 porosity and permeability reductions. No universally applicable model has been  
30 developed for saturated porous media systems. Moreover, no attempts have been made  
31 to develop a model that is applicable to both saturated and unsaturated systems. This  
32 situation could be particularly relevant to conditions that trigger gas generation as a

1 result of bacterial metabolic processes. Gas bubble formation and entrapment could also  
2 severely block the pore space. It is usually characteristic of denitrifying and  
3 methanogenic conditions where nitrogen (Soares et al., 1991) and methane gas  
4 (Beckwith and Baird, 2001) production is observed but not exclusively as CO<sub>2</sub> and  
5 other gases are produced as part of the metabolic processes of different species.  
6 Unsaturated conditions are crucial for understanding the flow and transport in  
7 environments such as groundwater recharge basins, bioremediation sites, and effluent  
8 irrigated fields. However, very few pore network models have been used to study the  
9 biofilm morphology under unsaturated conditions (Rosenzweig et al., 2013).  
10 Rosenzweig et al. proposed a pore network model of triangular channels to simulate  
11 variably saturated flows in biofilm-affected porous media. The effects of biofilm on the  
12 hydraulic properties of the network are demonstrated by examining three scenarios for  
13 the biofilm pore-scale morphology including plug (or microcolony) morphology and a  
14 uniform biofilm layer (Rosenzweig et al., 2013). The simulations demonstrated that the  
15 effect of biofilms on the hydraulic properties of the network is a complicated and  
16 nonlinear function that depends not only on the biofilm scenario but also on the  
17 saturation.

18

19 A significant assumption in most existing biofilm simulation models is that biofilm-  
20 occupied regions are impermeable and that nutrient provision within the biofilm is  
21 purely as a result of diffusion. However, experimental studies have demonstrated that  
22 biofilm morphology is often extremely heterogeneous and can contain voids (e.g.,  
23 (Flemming et al., 2000)). As a result, biofilms are not fully impermeable and can  
24 contain a significant amount of both static and dynamic water (Flemming et al., 2000).  
25 In the absence of biofilm detachment, the effect of permeability is only relevant when  
26 biofilm growth is nutrient mass transfer limited. Such conditions are prominent in  
27 subsurface conditions (Kim and Fogler, 2000) and are very relevant to bio-barrier  
28 scenarios where thick biofilms are desirable for permeability reduction. Thullner et al.  
29 studied the effects of permeability of biofilms on the hydraulic conductivity of porous  
30 media by pore network models (Thullner and Baveye, 2008). The computational pore  
31 network model consisted of cylindrical pores which were arranged in an orthogonal  
32 array in two or three dimensions. The nodes connecting adjacent pores are assumed to

1 be volumeless. The biofilm is viewed as homogeneous with regard to its hydraulic and  
2 biological characteristics in the model. In each pore, microbial activity is assumed to  
3 take place exclusively within the biofilm. This model was able to simulate reductions of  
4 the hydraulic conductivity of the pore networks by two to three orders of magnitudes.  
5 These reductions are in good agreement with laboratory experiments with sand columns  
6 or field situations (Thullner and Baveye, 2008). The amount of biomass in any given  
7 pore is controlled by biomass growth, decay processes inside the biofilm, and  
8 detachment of biomass due to shear forces. However, few pore network models  
9 simulate all the biomass growth or surface attachment mechanisms.

## 11 **5. Discussion and conclusions**

13 The paper reviewed three aspects of pore network modelling: main experimental  
14 techniques for characterisation of pore spaces; main methods for construction of pore  
15 networks reflecting available pore space characteristics; and application of pore network  
16 models to analysis of phenomena, which have not been covered in previous reviews –  
17 sorption, dissolution and biofilm growth – but have increasing technological and  
18 scientific importance. The works reviewed demonstrate that pore network modelling is  
19 an efficient and useful approach to analysis of reactive transport at the meso-scale, less  
20 computationally demanding than direct methods and able to incorporate heterogeneity  
21 within larger rock volumes.

23 In many practical cases, the main source of uncertainty in pore space characterisation is  
24 the finite resolution of the imaging techniques. These contain a hierarchy of pores from  
25 nanometres to micrometres. The uncertainties could arise from hardware limitations or  
26 from compromising resolution to capture heterogeneities. The errors may arise from the  
27 relatively sparse numerical grid of the imaging techniques, whereby details of the  
28 structure, e.g. very narrow passages in the porous space and surface roughness of fibres,  
29 may not be reproduced by the images. Furthermore, the results for each individual  
30 sample may be affected by the methods used to minimise or remove noise and other  
31 artefacts present in the original reconstructed images. These are the main factors that  
32 currently limit the applicability of the imaging techniques especially for fine-structured

1 materials. The limitation is particularly relevant to materials with tight pore spaces, such  
2 as clays and cement-based materials. For example in concrete, the so-called air porosity  
3 can be resolved by existing methods, but appears as disconnected set of pores. The  
4 transport pathways are formed by the gel porosity of the cement, as well as along the so-  
5 called interfacial transitions zones between cement and aggregates, the connectivity of  
6 which is not resolvable with the current techniques. Similar is the situation with  
7 compacted clays. In such cases, the connectivity of the transport pathways needs to be  
8 assumed and tested against macroscopic transport experiments until suitable  
9 connectivity is found (Xiong et al., 2015).

10  
11 In addition to numerical uncertainties arising from discretisation and image quality  
12 discussed above, this deviation includes statistical variation arising from relatively small  
13 size and low number of samples used in computation. In principle, the accuracy can be  
14 improved by using higher resolution images and better statistics. The former condition  
15 may become feasible with the present rapid development of imaging techniques. The  
16 latter can be obtained by larger size or larger number of samples. Clearly, these  
17 improvements come with the cost of higher computational effort, which, however, does  
18 not appear critical from the point of view of applicability of the method. Another  
19 approach for overcoming the above mentioned problems is to use a combination of  
20 different techniques such as FIB/SEM, nitrogen adsorption and FIB (Keller et al., 2013).

21  
22 It must be noted that pore network modelling is conceptually scale indifferent, i.e. the  
23 approach can be applied to any length interval, where the structure of the pore space has  
24 been experimentally observed and analysed. For example if a particular experimental  
25 technique allows for characterising pore features of sizes between  $0.1\mu\text{m}$  and  $10\mu\text{m}$ ,  
26 then the corresponding PNM will take these into account. The elements of PNM, sites  
27 and bonds, are abstract and can be related to the measurable features in different ways  
28 depending on the available information. The individual pore networks can be extracted  
29 at each length scale and then integrated into a single multi-scale network by  
30 characterizing the cross-scale connection structure between these networks (Bultreys et  
31 al., 2015; Jiang et al., 2013).



1 Pore network models have been proven to be an effective research tool to upscale  
2 reactive transport processes from the local scale to the continuum scale. The  
3 microscopic dynamics can be understood best at the scale of individual pores. It is  
4 challenging to directly correlate results obtained from pore scale simulations to improve  
5 quantitative predictions based on large-scale simulations. However, the results obtained  
6 from pore scale investigations contribute to the understanding of large-scale natural  
7 processes and improve large scale geotechnical applications. It is well known that some  
8 large scale reactive process may be difficult to predict or explain unless there is a well  
9 defined experiment that has been used to study it precisely. Pore network models allow  
10 for bridging the gap between laboratory simulations and larger scale transport. Although  
11 pore scale is difficult to evaluate with traditional experimental studies, detailed  
12 investigations allow for the identification of important pore-structure details that are  
13 essential and control the reactive transport processes at the engineering/continuum scale.

14  
15 It should be mentioned that, in spite of the attractiveness and successful applications of  
16 pore network models, as any other numerical method they have certain limitations. First  
17 of all, successful simulation of transport requires adequate representation of the real  
18 porous media. Pore network models usually simplify the geometry of the pore space and  
19 sometimes cannot capture all characteristics due to lack of resolution in most  
20 simulations. Whether the pore networks could reasonably predict single and multi phase  
21 properties depends on whether all relevant details are identified and included. In many  
22 systems, the very small pores below the image resolution make a little contribution to  
23 the overall behaviour. In these cases, transport properties are well predicted when the  
24 principal connected pore space is modelled, while the smaller pores could be neglected.  
25 Otherwise, assumptions are required. Secondly, the detailed microscopic features, such  
26 as the exact molecular structures and intermolecular interactions cannot be represented  
27 explicitly in pore network models. Therefore, in such situations, many approaches have  
28 been developed to study upscaling reactive transport in porous media (Algive et al.,  
29 2010; Li et al., 2006; Varloteaux et al., 2013). Reactive transport processes are  
30 simulated at the pore scale, which allows for incorporation of physical and chemical  
31 effects' rate variations from pore to pore. The reactive transport is then upscaled from  
32 the pore scale to a heterogeneous porous medium with the aid of a sufficiently large

1 three-dimensional pore network model. The PNM is used to determine the  
2 phenomenological transport coefficients and the porosity/permeability relationship,  
3 which can be used as inputs in reservoir scale simulation (Algive et al., 2010; Li et al.,  
4 2006; Varloteaux et al., 2013). The strength of the pore network models is that they can  
5 be developed elegantly to study the effect of pore space changing mechanisms. In most  
6 simulations of pore-scale mass transport the pore geometry is assumed to be constant,  
7 apart from the effects of reaction. However, in many important geo-systems the  
8 confining geometry changes slowly as a result of processes such as pressure solution  
9 (Tada and Siever, 1989) or rapidly because of fracturing and changes in pore pressure or  
10 matrix stress. It is important to include the coupling between diffusion and geo-  
11 mechanical processes for a number of important applications including oil recovery and  
12 carbon dioxide sequestration.

13

14 Modelling and simulation of mineral precipitation and dissolution on the pore-scale  
15 have not been subjects to extensive research in the geo-science community. In particular,  
16 most simulations have employed very simple models for dissolution and/or precipitation  
17 chemistry, and there has been little, if any, work on chemical processes coupled with  
18 multiphase diffusion. It is believed that this situation is likely to change rapidly. There  
19 is strong motivation for such simulations for both scientific discovery and practical  
20 applications. Furthermore, the simulated results are usually compared with experimental  
21 data, which will not give the same results realistically. For example, in the reactive  
22 diffusion, a small change in the pore space geometry can lead to a large change in the  
23 fluid-solid interface. Similarly, micro-scale roughness and trace impurities can also have  
24 a strong impact on the outcome of experiments. Consequently, experimental validation  
25 of computer models for reactive transport in porous media must be based primarily on  
26 the comparison of statistical measures such as correlation functions, saturations, etc.

27

## 28 **Acknowledgements**

29 Xiong acknowledges gratefully the support of the President of The University of  
30 Manchester through the Doctoral Award Scheme. Baychev acknowledges the support of  
31 EPSRC via Nuclear FiRST Doctoral Training Centre, Grant EP/G037140/1. Jivkov  
32 acknowledges the support of EPSRC via grant EP/K016946/1, “Graphene-based

1 membranes”, of EdF R&D for the Modelling & Simulation Centre, and of BNFL for the  
2 Research Centre for Radwaste & Decommissioning.

#### 4 **References**

5 Abichou, T., Benson, C.H. and Edil, T.B., 2004. Network model for hydraulic  
6 conductivity of sand-bentonite mixtures. *Canadian Geotechnical Journal*, 41(4):  
7 698-712.

8 Acharya, R., Van der Zee, S. and Leijnse, A., 2005. Transport modeling of nonlinearly  
9 adsorbing solutes in physically heterogeneous pore networks. *Water Resources*  
10 *Research*, 41(2).

11 Adler, P. and Thovert, J.-F., 1998. Real porous media: Local geometry and macroscopic  
12 properties. *Applied Mechanics Reviews*, 51(9): 537-585.

13 Akratanakul, S., Boersma, L. and Klock, G., 1983. Sorption processes in soils as  
14 influenced by pore water velocity: 2. Experimental results. *Soil Science*, 135(6):  
15 331-341.

16 Al-Gharbi, M.S. and Blunt, M.J., 2005. Dynamic network modeling of two-phase  
17 drainage in porous media. *Physical Review E*, 71(1): 016308.

18 Al-Kharusi, A.S. and Blunt, M.J., 2007. Network extraction from sandstone and  
19 carbonate pore space images. *Journal of Petroleum Science and Engineering*,  
20 56(4): 219-231.

21 Al-Raoush, R., Thompson, K. and Willson, C.S., 2003. Comparison of network  
22 generation techniques for unconsolidated porous media. *Soil Science Society of*  
23 *America Journal*, 67(6): 1687-1700.

24 Al-Raoush, R. and Willson, C., 2005. Extraction of physically realistic pore network  
25 properties from three-dimensional synchrotron X-ray microtomography images  
26 of unconsolidated porous media systems. *Journal of Hydrology*, 300(1): 44-64.

27 Algive, L., Bekri, S. and Vizika, O., 2010. Pore-network modeling dedicated to the  
28 determination of the petrophysical-property changes in the presence of reactive  
29 fluid. *SPE Journal*, 15(03): 618-633.

30 AMS, C.H., KNACKSTEDT, M.A., VAL PINCZEWSKI, W. and MARTYS, N.S.,  
31 2004. Virtual permeametry on microtomographic images. *Journal of petroleum*  
32 *science & engineering*, 45(1-2): 41-46.

- 1 Appelo, C.A.J., Van Loon, L.R. and Wersin, P., 2010. Multicomponent diffusion of a  
2 suite of tracers (HTO, Cl, Br, I, Na, Sr, Cs) in a single sample of Opalinus Clay.  
3 *Geochimica et Cosmochimica Acta*, 74(4): 1201-1219.
- 4 Aytas, S., Yurtlu, M. and Donat, R., 2009. Adsorption characteristic of U(VI) ion onto  
5 thermally activated bentonite. *Journal of Hazardous Materials*, 172(2-3): 667-74.
- 6 Bakke, S. and Oren, P.-E., 1997. 3-D pore-scale modelling of sandstones and flow  
7 simulations in the pore networks. *SPE JOURNAL-RICHARDSON*-, 2: 136-149.
- 8 Baldwin, C.A., Sederman, A.J., Mantle, M.D., Alexander, P. and Gladden, L.F., 1996.  
9 Determination and characterization of the structure of a pore space from 3D  
10 volume images. *Journal of Colloid and Interface Science*, 181(1): 79-92.
- 11 Balhoff, M.T. and Wheeler, M.F., 2009. A predictive pore-scale model for non-Darcy  
12 flow in porous media. *SPE Journal*, 14(04): 579-587.
- 13 Barrett, E.P., Joyner, L.G. and Halenda, P.P., 1951. The determination of pore volume  
14 and area distributions in porous substances. I. Computations from nitrogen  
15 isotherms. *Journal of the American Chemical Society*, 73(1): 373-380.
- 16 Bauer, D. et al., 2012. Improving the estimations of petrophysical transport behavior of  
17 carbonate rocks using a dual pore network approach combined with computed  
18 microtomography. *Transport in Porous Media*, 94(2): 505-524.
- 19 Beckwith, C.W. and Baird, A.J., 2001. Effect of biogenic gas bubbles on water flow  
20 through poorly decomposed blanket peat. *Water Resources Research*, 37(3):  
21 551-558.
- 22 Bekri, S., Laroche, C. and Vizika, O., 2005. Pore network models to calculate transport  
23 and electrical properties of single or dual-porosity rocks, *International*  
24 *Symposium of the Society of Core Analysts*, Toronto.
- 25 Bhattad, P., Willson, C.S. and Thompson, K.E., 2011. Effect of network structure on  
26 characterization and flow modeling using X-ray micro-tomography images of  
27 granular and fibrous porous media. *Transport in porous media*, 90(2): 363-391.
- 28 Biswal, B., Manwart, C., Hilfer, R., Bakke, S. and Øren, P., 1999. Quantitative analysis  
29 of experimental and synthetic microstructures for sedimentary rock. *Physica A:*  
30 *Statistical Mechanics and its Applications*, 273(3): 452-475.
- 31 Blümich, B., Casanova, F. and Appelt, S., 2009. NMR at low magnetic fields. *Chemical*  
32 *Physics Letters*, 477(4): 231-240.

- 1 Blunt, M.J. et al., 2013. Pore-scale imaging and modelling. *Advances in Water*  
2 *Resources*, 51: 197-216.
- 3 Blunt, M.J., Jackson, M.D., Piri, M. and Valvatne, P.H., 2002. Detailed physics,  
4 predictive capabilities and macroscopic consequences for pore-network models  
5 of multiphase flow. *Advances in Water Resources*, 25(8): 1069-1089.
- 6 Blunt, M.J., King, M.J. and Scher, H., 1992. Simulation and theory of two-phase flow in  
7 porous media. *Physical Review A*, 46(12): 7680.
- 8 Boulton, K. et al., 1998. Towards an understanding of the sorption of U (VI) and Se (IV)  
9 on sodium bentonite. *Journal of Contaminant Hydrology*, 35(1): 141-150.
- 10 Bourg, I.C., Bourg, A.C.M. and Sposito, G., 2003. Modeling diffusion and adsorption in  
11 compacted bentonite: a critical review. *Journal of Contaminant Hydrology*,  
12 61(1-4): 293-302.
- 13 Bourg, I.C., Sposito, G. and Bourg, A.C., 2006. Tracer diffusion in compacted, water-  
14 saturated bentonite. *Clays and Clay Minerals*, 54(3): 363-374.
- 15 Bradbury, M.H. and Baeyens, B., 2003. Porewater chemistry in compacted re-saturated  
16 MX-80 bentonite. *Journal of Contaminant Hydrology*, 61(1): 329-338.
- 17 Broekhoff, J. and De Boer, J., 1967. Studies on pore systems in catalysts: IX.  
18 Calculation of pore distributions from the adsorption branch of nitrogen sorption  
19 isotherms in the case of open cylindrical pores A. Fundamental equations.  
20 *Journal of Catalysis*, 9(1): 8-14.
- 21 Brunauer, S., Emmett, P.H. and Teller, E., 1938. Adsorption of gases in multimolecular  
22 layers. *Journal of the American Chemical Society*, 60(2): 309-319.
- 23 Brusseau, M.L., 1992. Nonequilibrium transport of organic chemicals: The impact of  
24 pore-water velocity. *Journal of Contaminant Hydrology*, 9(4): 353-368.
- 25 Bryant, S.L. and Blunt, M.J., 1992. Prediction of relative permeability in simple porous  
26 media. *Physical Review A*, 46(4): 2004.
- 27 Bryant, S.L., King, P.R. and Mellor, D.W., 1993a. Network model evaluation of  
28 permeability and spatial correlation in a real random sphere packing. *Transport*  
29 *in Porous Media*, 11(1): 53-70.
- 30 Bryant, S.L., Mellor, D.W. and Cade, C.A., 1993b. Physically representative network  
31 models of transport in porous media. *AIChE Journal*, 39(3): 387-396.

- 1 Bryntesson, L.M., 2002. Pore network modelling of the behaviour of a solute in  
2 chromatography media: transient and steady-state diffusion properties. *Journal*  
3 *of Chromatography A*, 945(1): 103-115.
- 4 Bultreys, T., Van Hoorebeke, L. and Cnudde, V., 2015. Multi-scale, micro-computed  
5 tomography-based pore network models to simulate drainage in heterogeneous  
6 rocks. *Advances in Water Resources*, 78(0): 36-49.
- 7 Callaghan, P.T., 1993. *Principles of nuclear magnetic resonance microscopy*. Oxford  
8 University Press on Demand.
- 9 Câmara, L.D.T. and Silva Neto, A.J., 2009. Network modeling of chromatography by  
10 stochastic phenomena of adsorption, diffusion and convection. *Applied*  
11 *Mathematical Modelling*, 33(5): 2491-2501.
- 12 Cazorla-Amorós, D., Alcaniz-Monge, J., De la Casa-Lillo, M. and Linares-Solano, A.,  
13 1998. CO<sup>2</sup> as an adsorptive to characterize carbon molecular sieves and  
14 activated carbons. *Langmuir*, 14(16): 4589-4596.
- 15 Christenson, H.K., 2001. Confinement effects on freezing and melting. *Journal of*  
16 *Physics: Condensed Matter*, 13(11): R95.
- 17 Coelho, D., Thovert, J.-F. and Adler, P., 1997. Geometrical and transport properties of  
18 random packings of spheres and aspherical particles. *Physical Review E*, 55:  
19 1959-1978.
- 20 Crandell, L.E., Peters, C.A., Um, W., Jones, K.W. and Lindquist, W.B., 2012. Changes  
21 in the pore network structure of Hanford sediment after reaction with caustic  
22 tank wastes. *Journal of Contaminant Hydrology*, 131(1-4): 89-99.
- 23 Cunningham, A.B., Characklis, W.G., Abedeen, F. and Crawford, D., 1991. Influence  
24 of biofilm accumulation on porous media hydrodynamics. *Environmental*  
25 *Science & Technology*, 25(7): 1305-1311.
- 26 Curtis, M.E., Ambrose, R.J. and Sondergeld, C.H., 2010. Structural characterization of  
27 gas shales on the micro-and nano-scales, Canadian unconventional resources  
28 and international petroleum conference. Society of Petroleum Engineers.
- 29 De Josselin de Jong, G., 1958. Longitudinal and transverse diffusion in granular  
30 deposits. *Transactions, American Geophysical Union*, 39: 67-74.

- 1 Dillard, L.A. and Blunt, M.J., 2000. Development of a pore network simulation model  
2 to study nonaqueous phase liquid dissolution. *Water Resources Research*, 36(2):  
3 439-454.
- 4 Dong, H. and Blunt, M.J., 2009. Pore-network extraction from micro-computerized-  
5 tomography images. *Physical Review E*, 80(3): 036307.
- 6 Dupin, H.J., Kitanidis, P.K. and McCarty, P.L., 2001a. Pore-scale modeling of  
7 biological clogging due to aggregate expansion: A material mechanics approach.  
8 *Water Resources Research*, 37(12): 2965-2979.
- 9 Dupin, H.J., Kitanidis, P.K. and McCarty, P.L., 2001b. Simulations of two-dimensional  
10 modeling of biomass aggregate growth in network models. *Water Resources*  
11 *Research*, 37(12): 2981-2994.
- 12 Dupin, H.J. and McCarty, P.L., 2000. Impact of colony morphologies and disinfection  
13 on biological clogging in porous media. *Environmental science & technology*,  
14 34(8): 1513-1520.
- 15 Ezeuko, C., Sen, A., Grigoryan, A. and Gates, I., 2011. Pore - network modeling of  
16 biofilm evolution in porous media. *Biotechnology and Bioengineering*, 108(10):  
17 2413-2423.
- 18 Fatt, I., 1956. The network model of porous media. *Trans AIME*, 207: 144–159.
- 19 Fenwick, D. and Blunt, M.J., 1998. Network modeling of three-phase flow in porous  
20 media. *SPE Journal*, 3(1): 86-96.
- 21 Flemming, H.-C., Szewzyk, U. and Griebe, T., 2000. *Biofilms: investigative methods*  
22 *and applications*. CRC Press.
- 23 Gao, S., Meegoda, J.N. and Hu, L., 2012. Two methods for pore network of porous  
24 media. *International Journal for Numerical and Analytical Methods in*  
25 *Geomechanics*, 36(18): 1954-1970.
- 26 Gharasoo, M., Centler, F., Regnier, P., Harms, H. and Thullner, M., 2012. A reactive  
27 transport modeling approach to simulate biogeochemical processes in pore  
28 structures with pore-scale heterogeneities. *Environmental Modelling & Software*,  
29 30: 102-114.
- 30 Ghassemi, A. and Pak, A., 2011. Pore scale study of permeability and tortuosity for  
31 flow through particulate media using lattice Boltzmann method. *International*  
32 *Journal for Numerical and Analytical Methods in Geomechanics*, 35(8): 886-901.

- 1 Giesche, H., 2006. Mercury porosimetry: a general (practical) overview. *Particle &*  
2 *Particle Systems Characterization*, 23(1): 9-19.
- 3 Glantz, R. and Hilpert, M., 2007. Dual models of pore spaces. *Advances in water*  
4 *resources*, 30(2): 227-248.
- 5 Glantz, R. and Hilpert, M., 2008. Tight dual models of pore spaces. *Advances in water*  
6 *resources*, 31(5): 787-806.
- 7 Groen, J.C., Peffer, L.A. and Pérez-Ramírez, J., 2003. Pore size determination in  
8 modified micro-and mesoporous materials. Pitfalls and limitations in gas  
9 adsorption data analysis. *Microporous and Mesoporous Materials*, 60(1): 1-17.
- 10 Hao, L. and Cheng, P., 2010. Pore-scale simulations on relative permeabilities of porous  
11 media by lattice Boltzmann method. *International Journal of Heat and Mass*  
12 *Transfer*, 53(9): 1908-1913.
- 13 Hazlett, R., 1995. Simulation of capillary-dominated displacements in  
14 microtomographic images of reservoir rocks. *Transport in Porous Media*, 20(1-  
15 2): 21-35.
- 16 Hilfer, R., 1991. Geometric and dielectric characterization of porous media. *Physical*  
17 *Review B*, 44(1): 60.
- 18 Horvath, G. and Kawazoe, K., 1983. Method for the calculation of effective pore size  
19 distribution in molecular sieve carbon. *Journal of Chemical Engineering of*  
20 *Japan*, 16(6): 470-475.
- 21 Hui, M.-H. and Blunt, M.J., 2000. Effects of wettability on three-phase flow in porous  
22 media. *The Journal of Physical Chemistry B*, 104(16): 3833-3845.
- 23 Ioannidis, M. and Chatzis, I., 2000. On the geometry and topology of 3D stochastic  
24 porous media. *Journal of Colloid and Interface Science*, 229(2): 323-334.
- 25 Ioannidis, M.A. and Chatzis, I., 1993a. A mixed-percolation model of capillary  
26 hysteresis and entrapment in mercury porosimetry. *Journal of Colloid and*  
27 *Interface Science*, 161(2): 278-291.
- 28 Ioannidis, M.A. and Chatzis, I., 1993b. Network modelling of pore structure and  
29 transport properties of porous media. *Chemical Engineering Science*, 48(5): 951-  
30 972.
- 31 Jacob, B., 1972. *Dynamics of fluids in porous media*. American Elsevier



- 1 Jiang, Z., Dijke, M., Sorbie, K. and Couples, G., 2013. Representation of multiscale  
2 heterogeneity via multiscale pore networks. *Water Resources Research*, 49(9):  
3 5437-5449.
- 4 Jiang, Z. et al., 2007. Efficient extraction of networks from three - dimensional porous  
5 media. *Water Resources Research*, 43(12).
- 6 Jivkov, A.P., Gunther, M. and Travis, K.P., 2012. Site-bond modelling of porous quasi-  
7 brittle media. *Mineralogical Magazine*, 76(8): 2969-2974.
- 8 Jivkov, A.P., Hollis, C., Etiese, F., McDonald, S.A. and Withers, P.J., 2013. A novel  
9 architecture for pore network modelling with applications to permeability of  
10 porous media. *Journal of Hydrology*, 486: 246-258.
- 11 Jivkov, A.P. and Olele, J.E., 2012. Novel lattice models for porous media, *MRS*  
12 *Proceedings*. Cambridge Univ Press, pp. imrc11-1475-nw35-o62.
- 13 Jivkov, A.P. and Xiong, Q., 2014. A Network Model for Diffusion in Media with  
14 Partially Resolvable Pore Space Characteristics. *Transport in Porous Media*,  
15 105(1): 83-104.
- 16 Kang, Q., Lichtner, P.C., Viswanathan, H.S. and Abdel-Fattah, A.I., 2010. Pore scale  
17 modeling of reactive transport involved in geologic CO<sup>2</sup> sequestration.  
18 *Transport in Porous Media*, 82(1): 197-213.
- 19 Keller, L.M. et al., 2011. On the application of focused ion beam nanotomography in  
20 characterizing the 3D pore space geometry of Opalinus clay. *Physics and*  
21 *Chemistry of the Earth, Parts A/B/C*, 36(17): 1539-1544.
- 22 Keller, L.M. et al., 2013. Characterization of multi-scale microstructural features in  
23 Opalinus Clay. *Microporous and Mesoporous Materials*, 170: 83-94.
- 24 Ketcham, R.A. and Carlson, W.D., 2001. Acquisition, optimization and interpretation of  
25 X-ray computed tomographic imagery: applications to the geosciences.  
26 *Computers & Geosciences*, 27(4): 381-400.
- 27 Kikkinides, E. and Politis, M., 2014. Linking pore diffusivity with macropore structure  
28 of zeolite adsorbents. Part II: simulation of pore diffusion and mercury intrusion  
29 in stochastically reconstructed zeolite adsorbents. *Adsorption*, 20(1): 21-35.
- 30 Kim, D.-S. and Fogler, H.S., 2000. Biomass evolution in porous media and its effects  
31 on permeability under starvation conditions.

- 1 Kim, D. and Lindquist, W.B., 2013. Effects of network dissolution changes on pore -  
2 to - core upscaled reaction rates for kaolinite and anorthite reactions under  
3 acidic conditions. *Water Resources Research*, 49(11): 7575-7586.
- 4 Kim, D., Peters, C. and Lindquist, W., 2011a. Upscaling geochemical reaction rates  
5 accompanying acidic CO<sup>2</sup>-saturated brine flow in sandstone aquifers. *Water*  
6 *Resources Research*, 47(1).
- 7 Kim, D., Peters, C. and Lindquist, W., 2011b. Upscaling geochemical reaction rates  
8 accompanying acidic CO<sub>2</sub> - saturated brine flow in sandstone aquifers. *Water*  
9 *Resources Research*, 47(1).
- 10 Knackstedt, M.A., Sheppard, A.P. and Pinczewski, W., 1998. Simulation of mercury  
11 porosimetry on correlated grids: Evidence for extended correlated heterogeneity  
12 at the pore scale in rocks. *Physical review E*, 58(6): R6923.
- 13 Knutson, C.E., Werth, C.J. and Valocchi, A.J., 2001. Pore - scale modeling of  
14 dissolution from variably distributed nonaqueous phase liquid blobs. *Water*  
15 *Resources Research*, 37(12): 2951-2963.
- 16 Kohler, M., Curtis, G.P., Kent, D.B. and Davis, J.A., 1996. Experimental investigation  
17 and modeling of Uranium (VI) transport under variable chemical conditions.  
18 *Water Resources Research*, 32(12): 3539-3551.
- 19 Kreft, J.-U., Picioreanu, C., Wimpenny, J.W. and van Loosdrecht, M.C., 2001.  
20 Individual-based modelling of biofilms. *Microbiology*, 147(11): 2897-2912.
- 21 Kwiecien, M., Macdonald, I. and Dullien, F., 1990. Three - dimensional reconstruction  
22 of porous media from serial section data. *Journal of Microscopy*, 159(3): 343-  
23 359.
- 24 Laudone, G.M., Matthews, G.P. and Gane, P.A.C., 2008. Modelling diffusion from  
25 simulated porous structures. *Chemical Engineering Science*, 63(7): 1987-1996.
- 26 Lemmens, H., Butcher, A. and Botha, P., 2010. FIB/SEM and automated mineralogy for  
27 core and cuttings analysis, SPE Russian Oil and Gas Conference and Exhibition.  
28 Society of Petroleum Engineers.
- 29 León y León, C.A., 1998. New perspectives in mercury porosimetry. *Advances in*  
30 *Colloid and Interface Science*, 76: 341-372.

- 1 Lerdahl, T.R., Oren, P.-E. and Bakke, S., 2000. A predictive network model for three-  
2 phase flow in porous media, SPE/DOE Improved Oil Recovery Symposium.  
3 Society of Petroleum Engineers.
- 4 Levitz, P., 1998. Off-lattice reconstruction of porous media: critical evaluation,  
5 geometrical confinement and molecular transport. *Advances in Colloid and*  
6 *Interface Science*, 76: 71-106.
- 7 Li, L., Peters, C. and Celia, M., 2007. Effects of mineral spatial distribution on reaction  
8 rates in porous media. *Water resources research*, 43(1).
- 9 Li, L., Peters, C.A. and Celia, M.A., 2006. Upscaling geochemical reaction rates using  
10 pore-scale network modeling. *Advances in water resources*, 29(9): 1351-1370.
- 11 Li, S.-G., Ruan, F. and McLaughlin, D., 1992. A space-time accurate method for  
12 solving solute transport problems. *Water Resources Research*, 28(9): 2297-2306.
- 13 Liang, Z., Fernandes, C., Magnani, F. and Philippi, P., 1998. A reconstruction technique  
14 for three-dimensional porous media using image analysis and Fourier transforms.  
15 *Journal of Petroleum Science and Engineering*, 21(3): 273-283.
- 16 Lindquist, W.B., Lee, S.M., Coker, D.A., Jones, K.W. and Spanne, P., 1996. Medial  
17 axis analysis of void structure in three-dimensional tomographic images of  
18 porous media. *Journal of Geophysical Research: Solid Earth (1978–2012)*,  
19 101(B4): 8297-8310.
- 20 Lindquist, W.B., Venkatarangan, A., Dunsmuir, J. and Wong, T.f., 2000. Pore and  
21 throat size distributions measured from synchrotron X - ray tomographic images  
22 of Fontainebleau sandstones. *Journal of Geophysical Research: Solid Earth*  
23 (1978–2012), 105(B9): 21509-21527.
- 24 Lopez, X., Valvatne, P.H. and Blunt, M.J., 2003. Predictive network modeling of  
25 single-phase non-Newtonian flow in porous media. *Journal of Colloid and*  
26 *Interface Science*, 264(1): 256-265.
- 27 Lukens, W.W., Schmidt-Winkel, P., Zhao, D., Feng, J. and Stucky, G.D., 1999.  
28 Evaluating pore sizes in mesoporous materials: a simplified standard adsorption  
29 method and a simplified Broekhoff-de Boer method. *Langmuir*, 15(16): 5403-  
30 5409.

- 1 Man, H. and Jing, X., 1999. Network modelling of wettability and pore geometry  
2 effects on electrical resistivity and capillary pressure. *Journal of Petroleum*  
3 *Science and Engineering*, 24(2): 255-267.
- 4 Manwart, C., Torquato, S. and Hilfer, R., 2000. Stochastic reconstruction of sandstones.  
5 *Physical Review E*, 62(1): 893.
- 6 Maraqa, M.A., Wallace, R.B. and Voice, T.C., 1999. Effects of residence time and  
7 degree of water saturation on sorption nonequilibrium parameters. *Journal of*  
8 *Contaminant Hydrology*, 36(1): 53-72.
- 9 McCarthy, J.F. and Zachara, J.M., 1989. Subsurface transport of contaminants.  
10 *Environmental Science & Technology*, 23(5): 496-502.
- 11 Meakin, P. and Tartakovsky, A.M., 2009. Modeling and simulation of pore-scale  
12 multiphase fluid flow and reactive transport in fractured and porous media.  
13 *Reviews of Geophysics*, 47(3).
- 14 Mehmani, A. and Prodanović, M., 2014. The effect of microporosity on transport  
15 properties in porous media. *Advances in Water Resources*, 63: 104-119.
- 16 Mehmani, Y., Sun, T., Balhoff, M., Eichhubl, P. and Bryant, S., 2012. Multiblock pore-  
17 scale modeling and upscaling of reactive transport: application to carbon  
18 sequestration. *Transport in Porous Media*, 95(2): 305-326.
- 19 Meyers, J. and Liapis, A., 1999. Network modeling of the convective flow and diffusion  
20 of molecules adsorbing in monoliths and in porous particles packed in a  
21 chromatographic column. *Journal of Chromatography A*, 852(1): 3-23.
- 22 Meyers, J., Nahar, S., Ludlow, D. and Liapis, A.I., 2001. Determination of the pore  
23 connectivity and pore size distribution and pore spatial distribution of porous  
24 chromatographic particles from nitrogen sorption measurements and pore  
25 network modelling theory. *Journal of Chromatography A*, 907(1): 57-71.
- 26 Michael D. Uchic, L.H., Beverley J. Inkson, Edward L. Principe and Paul Munroe, 2007.  
27 Three-Dimensional Microstructural Characterization Using Focused Ion Beam  
28 Tomography. *MRS BULLETIN* 32: 8.
- 29 Mitchell, J., Webber, J.B.W. and Strange, J.H., 2008. Nuclear magnetic resonance  
30 cryoporometry. *Physics Reports*, 461(1): 1-36.

1 Molz, F.J., Widdowson, M. and Benefield, L., 1986. Simulation of microbial growth  
2 dynamics coupled to nutrient and oxygen transport in porous media. *Water*  
3 *Resources Research*, 22(8): 1207-1216.

4 Neimark, A.V. and Ravikovitch, P.I., 2001. Capillary condensation in MMS and pore  
5 structure characterization. *Microporous and Mesoporous Materials*, 44: 697-707.

6 Neimark, A.V., Ravikovitch, P.I. and Vishnyakov, A., 2000. Adsorption hysteresis in  
7 nanopores. *Physical Review E*, 62(2): R1493.

8 Nogues, J.P., Fitts, J.P., Celia, M.A. and Peters, C.A., 2013. Permeability evolution due  
9 to dissolution and precipitation of carbonates using reactive transport modeling  
10 in pore networks. *Water Resources Research*, 49(9): 6006-6021.

11 Okabe, H. and Blunt, M.J., 2004. Prediction of permeability for porous media  
12 reconstructed using multiple-point statistics. *Physical Review E*, 70(6): 066135.

13 Or, D. and Tuller, M., 2000. Flow in unsaturated fractured porous media: Hydraulic  
14 conductivity of rough surfaces. *Water Resources Research*, 36(5): 1165-1177.

15 Oren, P.-E., 1994. Pore-scale network modelling of waterflood residual oil recovery by  
16 immiscible gas flooding. *SPE/DOE Improved Oil Recovery Symposium*.

17 Oren, P.-E. and Bakke, S., 2002. Process based reconstruction of sandstones and  
18 prediction of transport properties. *Transport in Porous Media*, 46(2-3): 311-343.

19 Oren, P.-E., Bakke, S. and Arntzen, O.J., 1998. Extending predictive capabilities to  
20 network models. *SPE Journal Richardson*, 3: 324-336.

21 Pang, L., Close, M., Schneider, D. and Stanton, G., 2002. Effect of pore-water velocity  
22 on chemical nonequilibrium transport of Cd, Zn, and Pb in alluvial gravel  
23 columns. *Journal of Contaminant Hydrology*, 57(3): 241-258.

24 Patzek, T. and Silin, D., 2001. Shape factor and hydraulic conductance in noncircular  
25 capillaries: I. One-phase creeping flow. *Journal of Colloid and Interface Science*,  
26 236(2): 295-304.

27 Payatakes, A.C., Tien, C. and Turian, R.M., 1973. A new model for granular porous  
28 media: Part I. Model formulation. *AIChE Journal*, 19(1): 58-67.

29 Picioreanu, C., Kreft, J.-U. and van Loosdrecht, M.C., 2004. Particle-based  
30 multidimensional multispecies biofilm model. *Applied and Environmental*  
31 *Microbiology*, 70(5): 3024-3040.

- 1 Pilotti, M., 2000. Reconstruction of clastic porous media. *Transport in Porous Media*,  
2 41(3): 359-364.
- 3 Pintelon, T., Graf von der Schulenburg, D. and Johns, M., 2009. Towards optimum  
4 permeability reduction in porous media using biofilm growth simulations.  
5 *Biotechnology and Bioengineering*, 103(4): 767-779.
- 6 Pintelon, T.R., Picioareanu, C., van Loosdrecht, M. and Johns, M.L., 2012. The effect of  
7 biofilm permeability on bio - clogging of porous media. *Biotechnology and*  
8 *Bioengineering*, 109(4): 1031-1042.
- 9 Prodanović, M., Lindquist, W. and Seright, R., 2006. Porous structure and fluid  
10 partitioning in polyethylene cores from 3D X-ray microtomographic imaging.  
11 *Journal of Colloid and Interface Science*, 298(1): 282-297.
- 12 Prodanović, M., Mehmani, A. and Sheppard, A.P., 2015. Imaged-based multiscale  
13 network modelling of microporosity in carbonates. Geological Society, London,  
14 *Special Publications*, 406(1): 95-113.
- 15 Raouf, A. and Hassanizadeh, S.M., 2010a. A new method for generating pore network  
16 models of porous media. *Transport in Porous Media*, 81(3): 391-407.
- 17 Raouf, A. and Hassanizadeh, S.M., 2010b. Upscaling transport of adsorbing solutes in  
18 porous media. *Journal of Porous Media*, 13(5).
- 19 Raouf, A., Nick, H., Hassanizadeh, S. and Spiers, C., 2013. PoreFlow: A complex pore-  
20 network model for simulation of reactive transport in variably saturated porous  
21 media. *Computers & Geosciences*, 61: 160-174.
- 22 Raouf, A., Nick, H.M., Wolterbeek, T.K.T. and Spiers, C.J., 2012. Pore-scale modeling  
23 of reactive transport in wellbore cement under CO<sub>2</sub> storage conditions.  
24 *International Journal of Greenhouse Gas Control*, 11, Supplement: S67-S77.
- 25 Ravikovitch, P.I., Vishnyakov, A., Russo, R. and Neimark, A.V., 2000. Unified  
26 approach to pore size characterization of microporous carbonaceous materials  
27 from N<sub>2</sub>, Ar, and CO<sub>2</sub> adsorption isotherms. *Langmuir*, 16(5): 2311-2320.
- 28 Rebuffel, V. and Dinten, J.-M., 2007. Dual-energy X-ray imaging: benefits and limits.  
29 *Insight-non-destructive testing and condition monitoring*, 49(10): 589-594.
- 30 Reeves, P.C. and Celia, M.A., 1996. A Functional Relationship Between Capillary  
31 Pressure, Saturation, and Interfacial Area as Revealed by a Pore-Scale Network  
32 Model. *Water Resources Research*, 32(8): 2345-2358.

- 1 Regnier, P., O'Kane, J.P., Steefel, C.I. and Vanderborght, J.P., 2002. Modeling complex  
2 multi-component reactive-transport systems: towards a simulation environment  
3 based on the concept of a Knowledge Base. *Applied Mathematical Modelling*,  
4 26(9): 913-927.
- 5 Ren, X., Wang, S., Yang, S. and Li, J., 2009. Influence of contact time, pH, soil  
6 humic/fulvic acids, ionic strength and temperature on sorption of U(VI) onto  
7 MX-80 bentonite. *Journal of Radioanalytical and Nuclear Chemistry*, 283(1):  
8 253-259.
- 9 Rittmann, B.E., 1993. The significance of biofilms in porous media. *Water Resources*  
10 *Research*, 29(7): 2195-2202.
- 11 Roberts, A. and Torquato, S., 1999. Chord-distribution functions of three-dimensional  
12 random media: approximate first-passage times of gaussian processes. *Physical*  
13 *Review E*, 59(5): 4953.
- 14 Rodriguez-Reinoso, F., 2009. Characterisation of Porous Solids VIII: Proceedings of  
15 the 8th International Symposium on the Characterisation of Porous Solids, 318.  
16 Royal Society of Chemistry.
- 17 Rolland du Roscoat, S. et al., 2014. Application of synchrotron X - ray  
18 microtomography for visualizing bacterial biofilms 3D microstructure in porous  
19 media. *Biotechnology and Bioengineering*, 111(6): 1265-1271.
- 20 Rosenzweig, R., Furman, A. and Shavit, U., 2013. A channel network model as a  
21 framework for characterizing variably saturated flow in biofilm-affected soils.  
22 *Vadose Zone Journal*, 12(2).
- 23 Rouquerol, J. et al., 2012. The characterization of macroporous solids: an overview of  
24 the methodology. *Microporous and Mesoporous Materials*, 154: 2-6.
- 25 Rouquerol, J., Rouquerol, F., Llewellyn, P., Maurin, G. and Sing, K.S., 2013.  
26 Adsorption by powders and porous solids: principles, methodology and  
27 applications. Academic press.
- 28 Ryazanov, A., van Dijke, M. and Sorbie, K., 2009. Two-phase pore network modelling:  
29 existence of oil layers during water invasion. *Transport in Porous Media*, 80(1):  
30 79-99.
- 31 Saito, A. and Foley, H., 1991. Curvature and parametric sensitivity in models for  
32 adsorption in micropores. *AIChE Journal*, 37(3): 429-436.

- 1 Saito, A. and Foley, H.C., 1995. Argon porosimetry of selected molecular sieves:  
2 experiments and examination of the adapted Horvath-Kawazoe model.  
3 *Microporous Materials*, 3(4): 531-542.
- 4 Schlüter, S., Sheppard, A., Brown, K. and Wildenschild, D., 2014. Image processing of  
5 multiphase images obtained via X-ray microtomography: A review. *Water*  
6 *Resources Research*, 50(4): 3615-3639.
- 7 Serrano, D. et al., 2009. Molecular and meso-and macroscopic properties of hierarchical  
8 nanocrystalline ZSM-5 zeolite prepared by seed silanization. *Chemistry of*  
9 *Materials*, 21(4): 641-654.
- 10 Shin, H., Lindquist, W., Sahagian, D. and Song, S.-R., 2005. Analysis of the vesicular  
11 structure of basalts. *Computers & Geosciences*, 31(4): 473-487.
- 12 Silin, D. and Patzek, T., 2006. Pore space morphology analysis using maximal inscribed  
13 spheres. *Physica A: Statistical Mechanics and its Applications*, 371(2): 336-360.
- 14 Sing, K., 2001. The use of nitrogen adsorption for the characterisation of porous  
15 materials. *Colloids and Surfaces A: Physicochemical and Engineering Aspects*,  
16 187-188: 3-9.
- 17 Soares, M.I.s.M., Braester, C., Belkin, S. and Abeliovich, A., 1991. Denitrification in  
18 laboratory sand columns: carbon regime, gas accumulation and hydraulic  
19 properties. *Water Research*, 25(3): 325-332.
- 20 Sok, R.M. et al., 2010. Pore scale characterization of carbonates at multiple scales:  
21 Integration of Micro-CT, BSEM, and FIBSEM. *Petrophysics*, 51(06).
- 22 Stewart, T.L. and Kim, D.-S., 2004. Modeling of biomass-plug development and  
23 propagation in porous media. *Biochemical Engineering Journal*, 17(2): 107-119.
- 24 Stewart, T.L. and Scott Fogler, H., 2002. Pore - scale investigation of biomass plug  
25 development and propagation in porous media. *Biotechnology and*  
26 *Bioengineering*, 77(5): 577-588.
- 27 Stingaciu, L. et al., 2010. Determination of pore size distribution and hydraulic  
28 properties using nuclear magnetic resonance relaxometry: A comparative study  
29 of laboratory methods. *Water Resources Research*, 46(11).
- 30 Stoodley, P., Boyle, J.D., DeBeer, D. and Lappin - Scott, H.M., 1999. Evolving  
31 perspectives of biofilm structure. *Biofouling*, 14(1): 75-90.



- 1 Strange, J.H., Rahman, M. and Smith, E., 1993. Characterization of porous solids by  
2 NMR. *Physical Review Letters*, 71(21): 3589.
- 3 Suchomel, B.J., Chen, B.M. and Allen III, M.B., 1998. Network model of flow,  
4 transport and biofilm effects in porous media. *Transport in Porous Media*, 30(1):  
5 1-23.
- 6 Tada, R. and Siever, R., 1989. Pressure solution during diagenesis. *Annual Review of*  
7 *Earth and Planetary Sciences*, 17: 89.
- 8 Tartakovsky, A.M. and Meakin, P., 2006. Pore scale modeling of immiscible and  
9 miscible fluid flows using smoothed particle hydrodynamics. *Advances in Water*  
10 *Resources*, 29(10): 1464-1478.
- 11 Tartakovsky, A.M., Meakin, P., Scheibe, T.D. and Eichler West, R.M., 2007.  
12 Simulations of reactive transport and precipitation with smoothed particle  
13 hydrodynamics. *Journal of Computational Physics*, 222(2): 654-672.
- 14 Taylor, S.W. and Jaffé P.R., 1990. Biofilm growth and the related changes in the  
15 physical properties of a porous medium: 1. Experimental investigation. *Water*  
16 *Resources Research*, 26(9): 2153-2159.
- 17 Thommes, M., 2010. Physical adsorption characterization of nanoporous materials.  
18 *Chem. Ing. Tech*, 82(7): 1059-1073.
- 19 Thommes, M., Köhn, R. and Fröba, M., 2002. Sorption and pore condensation behavior  
20 of pure fluids in mesoporous MCM-48 silica, MCM-41 silica, SBA-15 silica and  
21 controlled-pore glass at temperatures above and below the bulk triple point.  
22 *Applied Surface Science*, 196(1): 239-249.
- 23 Thommes, M., Smarsly, B., Groenewolt, M., Ravikovitch, P.I. and Neimark, A.V., 2006.  
24 Adsorption hysteresis of nitrogen and argon in pore networks and  
25 characterization of novel micro-and mesoporous silicas. *Langmuir*, 22(2): 756-  
26 764.
- 27 Thullner, M., 2010. Comparison of bioclogging effects in saturated porous media within  
28 one-and two-dimensional flow systems. *Ecological Engineering*, 36(2): 176-196.
- 29 Thullner, M. and Baveye, P., 2008. Computational pore network modeling of the  
30 influence of biofilm permeability on bioclogging in porous media.  
31 *Biotechnology and Bioengineering*, 99(6): 1337-1351.

- 1 Thullner, M., Schroth, M.H., Zeyer, J. and Kinzelbach, W., 2004. Modeling of a  
2 microbial growth experiment with bioclogging in a two-dimensional saturated  
3 porous media flow field. *Journal of Contaminant Hydrology*, 70(1): 37-62.
- 4 Thullner, M., Zeyer, J. and Kinzelbach, W., 2002. Influence of microbial growth on  
5 hydraulic properties of pore networks. *Transport in Porous Media*, 49(1): 99-122.
- 6 Tomutsa, L., Silin, D.B. and Radmilovic, V., 2007. Analysis of chalk petrophysical  
7 properties by means of submicron-scale pore imaging and modeling. *SPE*  
8 *Reservoir Evaluation & Engineering*, 10(03): 285-293.
- 9 Tsai, W.-F. and Chen, C.-J., 1995. Unsteady finite-analytic method for solute transport  
10 in ground-water flow. *Journal of Engineering Mechanics*, 121(2): 230-243.
- 11 Valckenborg, R., Pel, L. and Kopinga, K., 2002. Combined NMR cryoporometry and  
12 relaxometry. *Journal of Physics D: Applied Physics*, 35(3): 249.
- 13 Vandevivere, P. and Baveye, P., 1992. Saturated hydraulic conductivity reduction  
14 caused by aerobic bacteria in sand columns. *Soil Science Society of America*  
15 *Journal*, 56(1): 1-13.
- 16 Varloteaux, C., Békri, S. and Adler, P.M., 2013. Pore network modelling to determine  
17 the transport properties in presence of a reactive fluid: From pore to reservoir  
18 scale. *Advances in Water Resources*, 53: 87-100.
- 19 Vogel, H.-J. and Roth, K., 2001. Quantitative morphology and network representation  
20 of soil pore structure. *Advances in Water Resources*, 24(3): 233-242.
- 21 Vogel, H., 2000. A numerical experiment on pore size, pore connectivity, water  
22 retention, permeability, and solute transport using network models. *European*  
23 *Journal of Soil Science*, 51(1): 99-105.
- 24 Wang, X., Chen, C., Zhou, X., Tan, X. and Hu, W., 2005. Diffusion and sorption of U  
25 (VI) in compacted bentonite studied by a capillary method. *Radiochimica Acta*,  
26 93(5/2005): 273-278.
- 27 Wang, X., Yang, Z. and Jivkov, A.P., 2015a. Monte Carlo simulations of mesoscale  
28 fracture of concrete with random aggregates and pores: a size effect study.  
29 *Construction and Building Materials*, 80(0): 262-272.
- 30 Wang, X., Yang, Z., Yates, J.R., Jivkov, A.P. and Zhang, C., 2015b. Monte Carlo  
31 simulations of mesoscale fracture modelling of concrete with random aggregates  
32 and pores. *Construction and Building Materials*, 75(0): 35-45.

- 1 Wildenschild, D., Vaz, C., Rivers, M., Rikard, D. and Christensen, B., 2002a. Using X-  
2 ray computed tomography in hydrology: systems, resolutions, and limitations.  
3 Journal of Hydrology, 267(3): 285-297.
- 4 Wildenschild, D., Vaz, C.M.P., Rivers, M.L., Rikard, D. and Christensen, B.S.B., 2002b.  
5 Using X-ray computed tomography in hydrology: systems, resolutions, and  
6 limitations. Journal of Hydrology, 267(3-4): 285-297.
- 7 Wilkinson, D. and Willemsen, J.F., 1983. Invasion percolation: a new form of  
8 percolation theory. Journal of Physics A: Mathematical and General, 16(14):  
9 3365.
- 10 Wimpenny, J., Manz, W. and Szewzyk, U., 2000. Heterogeneity in biofilms. FEMS  
11 Microbiology Reviews, 24(5): 661-671.
- 12 Wirth, R., 2009. Focused Ion Beam (FIB) combined with SEM and TEM: Advanced  
13 analytical tools for studies of chemical composition, microstructure and crystal  
14 structure in geomaterials on a nanometre scale. Chemical Geology, 261(3): 217-  
15 229.
- 16 Withers, P.J., 2007. X-ray nanotomography. Materials Today, 10(12): 26-34.
- 17 Xiong, Q. and Jivkov, A.P., 2015. Analysis of pore structure effects on diffusive  
18 transport in Opalinus clay via pore network models. Mineralogical Magazine, in  
19 press.
- 20 Xiong, Q., Jivkov, A.P. and Ahmad, S.M., 2015a. Modelling reactive diffusion in clays  
21 with two-phase-informed pore networks. Applied Clay Science, in press.
- 22 Xiong, Q., Jivkov, A.P. and Yates, J.R., 2014. Discrete modelling of contaminant  
23 diffusion in porous media with sorption. Microporous and Mesoporous  
24 Materials, 185: 51-60.
- 25 Xiong, Q., Joseph, C., Schmeide, K. and Jivkov, A.P., 2015b. Measurement and  
26 modelling of reactive transport in engineered barriers for nuclear waste  
27 containment. Physical Chemistry Chemical Physics in press.
- 28 Yeong, C. and Torquato, S., 1998a. Reconstructing random media. Physical Review E,  
29 57(1): 495.
- 30 Yeong, C. and Torquato, S., 1998b. Reconstructing random media. II. Three-  
31 dimensional media from two-dimensional cuts. Physical Review E, 58(1): 224.

- 1 Yiotis, A.G., Tsimpanogiannis, I.N., Stubos, A.K. and Yortsos, Y.C., 2006. Pore-  
2 network study of the characteristic periods in the drying of porous materials.  
3 Journal of Colloid and Interface Science, 297(2): 738-748.
- 4 Zhang, M. and Jivkov, A., 2014. Microstructure-informed modelling of damage  
5 evolution in cement paste using a site-bond model. Construction and Building  
6 Materials, 66: 731-742.
- 7 Zhang, M., Xu, K., He, Y. and Jivkov, A.P., 2014. Pore-scale modelling of 3D moisture  
8 distribution and critical saturation in cementitious materials. Construction and  
9 Building Materials, 64: 222-230.
- 10 Zhang, M., Ye, G. and Breugel, K.V., 2013. Microstructure-based modeling of  
11 permeability of cementitious materials using multiple-relaxation-time lattice  
12 Boltzmann method. Computational Materials Science, 68: 142-151.
- 13 Zhang, X., Crawford, J.W. and Young, I.M., 2008. Does pore water velocity affect the  
14 reaction rates of adsorptive solute transport in soils? Demonstration with pore-  
15 scale modelling. Advances in Water Resources, 31(3): 425-437.
- 16 Zhou, D., Dillard, L.A. and Blunt, M.J., 2000. A physically based model of dissolution  
17 of nonaqueous phase liquids in the saturated zone. Transport in Porous Media,  
18 39(2): 227-255.
- 19 Zhu, Y. and Fox, P.J., 2002. Simulation of Pore-Scale Dispersion in Periodic Porous  
20 Media Using Smoothed Particle Hydrodynamics. Journal of Computational  
21 Physics, 182(2): 622-645.
- 22  
23  
24